Heliyon 10 (2024) e35278

Contents lists available at ScienceDirect

Heliyon

journal homepage: www.cell.com/heliyon

Research article

Probing *N*-substituted 4-(5-mercapto-4-ethyl-4H-1,2,4-triazol-3-yl)-*N*-phenylpiperdine-1-carboxamides as potent 15-LOX inhibitors supported with ADME, DFT calculations and molecular docking studies

Zahid Nawaz [a], Naheed Riaz [a,*], Muhammad Saleem [a], Ambar Iqbal [a,b], Syeda Abida Ejaz [c], Saima Muzaffar [d], Bushra Bashir [a], Muhammad Ashraf [a,**], Aziz-ur Rehman [e], Muhammad Sajjad Bilal [c], Bala Krishna Prabhala [f], Salvia Sajid [g]

[a] *Institute of Chemistry, Baghdad-ul-Jadeed Campus, The Islamia University of Bahawalpur, Bahawalpur, 63100, Pakistan*
[b] *Department of Biochemistry, Institute of Biochemistry, Biotechnology and Bioinformatics (IBBB), Baghdad-ul-Jadeed Campus, The Islamia University of Bahawalpur, Bahawalpur, 63100, Pakistan*
[c] *Department of Pharmaceutical Chemistry, Faculty of Pharmacy, Khawaja Fareed Campus, The Islamia University of Bahawalpur, Bahawalpur, 63100, Pakistan*
[d] *Department of Chemistry, Division of Sceience and Technology, University of Education, 54770, Lahore, Vehari Campus, Pakistan*
[e] *Department of Chemistry, Government College University Lahore, Lahore, 54000, Pakistan*
[f] *Institute of Physics, Chemistry and Pharmacy, University of Southern Denmark, Campusvej 55, 5230M, Denmark*
[g] *Department of Drug Design and Pharmacology, University of Copenhagen 2, DK-2100, Kobenhavn O, Denmark*

ARTICLE INFO

Keywords:
Azinanetriazole methylacetamides
Synthesis
Characterization
15-LOX inhibition
In silico studies
MTT assay
ADME studies
DFT calculations

ABSTRACT

In our continuous efforts to find out leads against the enzyme 15-lipoxygenase (15-LOX), the current study deals with the synthesis of a series of new *N*-alkyl/aralkyl/aryl derivatives of 2-(4-ethyl-5-(1-phenylcarbamoyl)piperidine-4H-1,2,4-triazol-3-ylthio)methylacetamide (**7a-n**) with anti-LOX activities. The synthesis was started by reacting phenylisocyanate with isonipecotate that sequentially converted into N-substituted ester (**1**), hydrazide (**2**), semicarbazide (**3**) and *N*-ethylated 5-(1-phenylcarbamoyl)piperidine-1,2,4-triazole (**4**). The final compounds, **7a-n,** were obtained by reacting **4** with various *N*-alkyl/aralkyl/aryl electrophiles. Both the intermediates and target compounds were characterized by FTIR, ^{1}H, ^{13}C NMR spectroscopy, EI-MS and HR-EI-MS spectrometry and screened against soybean 15-LOX by chemiluminescence method. The eight compounds **7e, 7j**, **7h, 7a, 7g, 7b, 7n, 7c** showed potent inhibitory activities against 15-LOX with values ranging from IC_{50} 0.36 ± 0.15 μM (**7e**) to IC_{50} 6.75 ± 0.17 μM (**7c**) compared with the reference quercetin (IC_{50} 4.86 ± 0.14 μM) and baicalein (IC_{50} 2.24 ± 0.13 μM). Two analogues (**7l, 7f**) had significantly outstanding inhibitory potential with IC_{50} values 12.15 ± 0.23 μM and 15.54 ± 0.26 μM, whereas, the derivatives **7i,** and **7d** displayed IC_{50} values of 21.56 ± 0.27 μM, 23.59 ± 0.24 μM and the compounds **7k, 7m** were found inactive. All analogues exhibited blood

* Corresponding author.
** Corresponding author.
E-mail addresses: lecturer.zahid@gmail.com (Z. Nawaz), nrch322@yahoo.com (N. Riaz), drsaleem_kr@yahoo.com (M. Saleem), ambar.iqbal@iub.edu.pk (A. Iqbal), abidaejaz2010@gmail.com (S.A. Ejaz), saimarao@ue.edu.pk (S. Muzaffar), b4bushra786@gmail.com (B. Bashir), dr.m.ashraf@gmail.com (M. Ashraf), azizryk@yahoo.com (A.-u. Rehman), khawajasajjad44@gmail.com (M.S. Bilal), bapra@sdu.dk (B.K. Prabhala), salvia.sajid@sund.ku.dk (S. Sajid).

https://doi.org/10.1016/j.heliyon.2024.e35278
Received 19 March 2024; Received in revised form 25 July 2024; Accepted 25 July 2024
Available online 29 July 2024

mononuclear cells (MNCs) viability >75 % at 0.25 mM concentration as determined by MTT method. Calculated pharmacokinetic properties projected good lipophilicity, bioavailability and drug-likeness properties and did not violate Lipinski's/Veber rule. Molecular docking studies revealed lower binding free energies of all the derivatives than the reference compounds. The binding free energies were −9.8 kcal/mol, −9.70 k/mol and −9.20 kcal/mol for **7j, 7h** and **7e**, respectively, compared with the standard quercetin (−8.47 kcal/mol) and baicalein (−8.98 kcal/mol). The docked ligands formed hydrogen bonds with the amino acid residues Gln598 (**7e**), Arg260, Val 126 (**7h**), Gln762, Gln574, Thr443, Arg580 (**7j**) while other hydrophobic interactions observed therein further stabilized the complexes. The results of density functional theory (DFT) revealed that analogues with more stabilized lower unoccupied molecular orbital (LUMO) had significant enzyme inhibitory activity. The data collectively supports these molecules as leads against 15-LOX and demand further investigations as anti-inflammatory agents.

1. Introduction

Inflammation is considered a passive process occurring due to the withdrawal of pro-inflammatory signals. When body cells are damaged or face external stimuli, cellular membrane phospholipids are hydrolyzed by phospholipase A_2 yielding arachidonic acid which is oxidized in cyclooxygenase (COX) and lipoxygenase (LOX) pathways to yield biologically active mediators of endocrine, autocrine and paracrine nature [1,2]. LOX-pathway involves a family of four enzymes (LOXs, EC 1.13.11.12) viz. 5-LOX, 8-LOX, 12-LOX, 15-LOX depending upon the double bond being oxidized in the reaction to produce the respective hydroperoxyeicosatetraenoic acid (HPETE) which are precursors of other secondary lipid mediators [2]. In case of 5-LOX, 5-HPETE is formed which is further oxidized to leukotriene A_4 (LTA_4) that subsequently yields LTB_4 by LTA_4 hydrolase. Most of these mediators are implicated in several disorders including asthma, arthritis, heart disease, colitis, diabetes mellitus, Alzheimer's disease and even in several types of cancers [3,4]. Human LOXs are differentially expressed in immune, endothelial and epithelial cells and play pivotal role in immunity, cell differentiation and skin barrier formation and, therefore, the biochemical properties of human LOXs are widely studied [1,5,6]. 15-LOX is involved in the promotion of cancer by amplifying peroxisome proliferator-activated receptor-gamma (PPARγ) [7]. The expression of 5-LOX, 12-LOX and 15-LOX is increased in asthma, atherosclerosis, neuroinflammation, neurodegenerative disorders and some types of cancers [8].

Human and plant LOXs possess the highest levels of sequence similarity in the catalytic domain and contain non-heme iron. It is well established that inhibitors of soybean 15-LOX are also good inhibitors for human 5-LOX [1,6]. The homology in sequences of LOX family members have hampered the development of specific inhibitors and no pharmaceutical product except zileuton (*N*-[1-(1-benzothien-2-yl)ethyl]-*N*-hydroxyurea) has been approved for the treatment of asthma [9]. Thus, there is continued interest for various LOX inhibitors as leads in search for anti-inflammatory agents.

A plethora of compounds have been reported as LOX inhibitors in search for leads for the development of anti-inflammatory agents to be used in the treatment of various inflammatory disorders [7,10–12]. Nitrogen and/or sulfur atoms containing heterocyclic compounds are of prime worth for medicinal chemists because they also bind DNA with hydrogen bonding and show anticancer and related activities with diverse medicinal applications [13,14]. Among others, triazoles are five membered three nitrogen atoms containing scaffolds with two isomers, that is, 1,2,3- and 1,2,4-triazoles, and occupy special place in drug discovery program. The aromaticity of the ring, resistance towards oxidation, reduction, hydrolysis and metabolic degradation are major features which assist in hydrogen bonding, dipole-dipole interactions and π-stacking interactions with diverse biological targets. 1,2,4-Triazole invent from pyrazole by replacing carbon at 4-position with N-atom and its integration in other heterocyclic structures induces compounds with potential exceptional pharmacological properties [15–23].

Nonetheless, 1,2,4-triazole analogues show an impressive array of activities, including antibacterial, antifungal, antitubercular, antioxidant, antitumor, analgesic, anti-inflammatory, and insecticidal properties [24–32]. The race to develop triazoles containing valuable substituents has ignited a fervent creative competition. 1,2,4-Triazole scaffold is present in several clinically used drugs like fluconazole, alprazolam, rizatriptan, trapidil, trazodone, and loreclezole, owing to its unique structural features. These compounds open new avenues for the development of analogues that manifest inhibitory potential towards various metabolic enzymes, such as metallo-*β*-lactamase, cyclooxygenase, glutathione *S*-transferase, tyrosinase, acetylcholinesterase, butyrylcholinesterase, monoamine oxidase, alkaline phosphatase, *α*-amylase, and *α*-glucosidase [28,33–44]. Given the significance of these findings, the objective of the recent work is to emphasize the need for continued exploration and development of novel 1,2,4-triazole analogues in the pursuit of promising lead compounds as potential anti-inflammatory agents.

1.1. Rationale of the work

A comprehensive literature review showed that piperidine scaffolds are implicated in preclinical and clinical testing as they demonstrate a variety of biological activities including anti-inflammatory, anticancer, antibacterial, antimalarial and antihypertensive [45]. As mentioned in Fig. 1, among several reported analogues, 3-(4-methoxyphenyl)-*N*-(2,4,4-trimethylpentane-2-yl)-6-phenylimidazo [2,1-b]thiazol-5-amine (**i**; IC_{50} 11.5 ± 0.78 μM) substantially inhibited LOX due to the strong network of hydrophobic interactions with the target moiety [46]. Pyrazole moiety is also reported as potent LOX inhibitor like 4-{3-amino-4-[(4-methylphenyl)-hydrazono]-5-imino-4,5-dihydropyrazol-1-yl}-benzenesulfonamide (**ii**; IC_{50} 1.92 ± 0.01 μM) [47].

In addition to this, compounds **iii** and **iv** in the Fig. 1 are recognized as potent LOX inhibitors with IC_{50} values of 2.79 ± 0.24 μM and 2.11 ± 0.006 μM, respectively. Their activity was due to the formation of hydrogen bonds between NH of 2-hydroxy aminopropoxy, O-atom of chromen ring and OH group of 2-hydroxy aminopropoxy that interacted with the active pocket of the target enzyme [48]. Indolylpyrazoline (**v**; IC_{50} 3.84 ± 0.01 μM) also displayed potent LOX inhibition wherein the pyrazoline ring substituted with 3-pyridyl moiety possessed lone pairs that were involved in binding interactions with the target enzyme. The phenyl ring of indole inhibitor was appropriately bound into the hydrophobic binding pocket with pyrazoline ring that was stabilized by the π-cation linkage [49]. Nevertheless, in another study, 3-methoxy substituent on the N-benzyl moiety with a *p*-tosyl group on the sulfonamide moiety of spiro [chromene-2,4′-piperidin]-6-amine (**vi**) was responsible for the improved inhibitory activity (Fig. 1) [50]. On the other hand, as mentioned in Fig. 1, triazole base heterocyclic analogues possessed potent LOX inhibitory profiles particularly the compounds (**vii,**

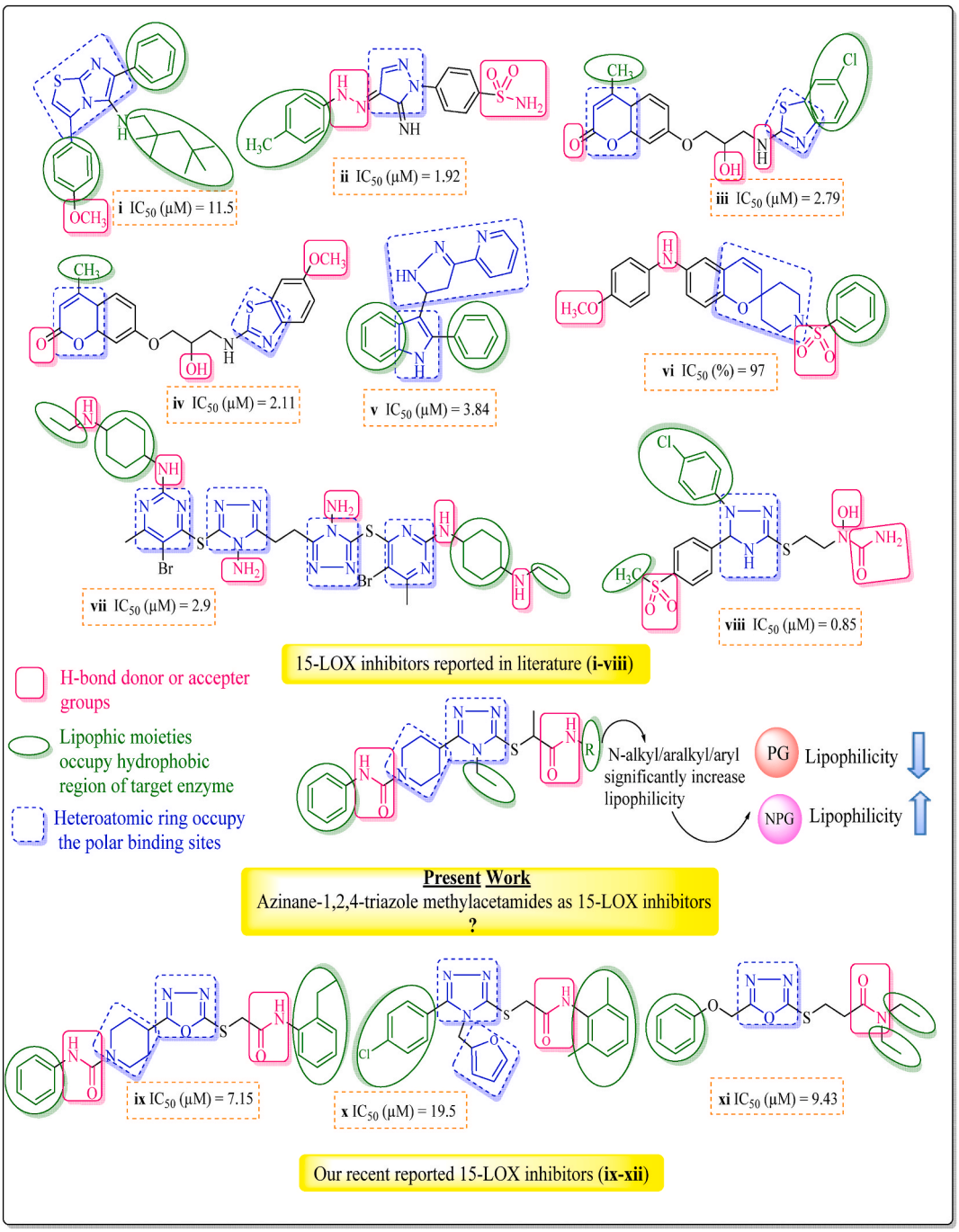

Fig. 1. Rationale of current research plan and reported LOX inhibitors.

viii; IC_{50} 2.9 μM and 0.85 ± 0.02 μM) which were equipped with electron rich substituents responsible for extraordinary activity [51, 52].

The above-mentioned importance of 1,2,4-triazoles as potent enzyme inhibitors describes the reason for the development of new compounds having triazole core. Considering this denotation, we published several papers on 1,2,4-triazoles and 1,3,4-oxadiazoles wherein the azinane ring and furfuryl groups were cohered and offered excellent 15-LOX inhibitory activities (**ix**, IC_{50} 7.15 ± 0.26 μM; **x**, IC_{50} 19.59 ± 0.83 μM; **xi**, IC_{50} 9.43 ± 0.17 μM; **xii**, IC_{50} 12.52 ± 0.35 μM) [53–55]. It is rationalized that hydrophobic terminals, heteroatoms and hydrogen bonding played major role to boost the LOX inhibitory activity. In our continuous efforts in search for new LOX inhibitors with triazole ring, the present study deals with the design and synthesis of a series of new *N*-alkyl/aralkyl/aryl triazole analogues (**7a-n**) with hydrophobic arms, more heteroatoms including maximum possibility of hydrogen donors and acceptors as powerful 15-LOX inhibitors using *in vitro* and *in silico* approaches.

2. Experimental

2.1. Materials & methods

The needed chemicals and solvents of analytical grade were vended from local retailer of Sigma, Aldrich and Alfa Aesar. The ^{1}H and ^{13}C NMR (Copenhagen, Denmark) spectra were recorded on Bruker instrument running at 400 and 100 MHz, respectively, employing tetramethylsilane as an internal standard. The IR (Copenhagen, Denmark) spectra were nailed on Shimadzu 460 FTIR spectro3meter using KBr disk. The mass spectra were attained on JMSA 500 mass spectrometer and JMS H × 110 spectrometer with data system. GallenKemp electro-thermal apparatus was used to garner melting points of synthesized derivatives. The reactions follow up and completions of reactions was monitored by thin layer chromatography (TLC).

2.2. Synthetic procedures

2.2.1. Synthesis of ethyl 1-phenylcarbamoylpiperidine-4-carboxylate (1)

Phenyl isocyanate (0.06 mol, 7.15 mL) was added dropwise to a watch glass having ethyl piperidine-4-carboxylate (**a**; 0.06 mol, 10 mL) with incessant rubbing, which further continued for 15–20 min until the development of one spot on TLC. The physical and spectroscopic data of **1** is as follows:

White solid; Yield: 99 %; M.P.: 107–110 °C; IR (KBr, ν_{max}, cm^{-1}): 3393 (N–H), 3038 (Ar–H), 2949 (C–H), 1732–1659 (C=O), 1613–1558 (Ar–C=C), 1261 (C–O, C–N); ^{1}H NMR (400 MHz, $CDCl_3$, ppm): δ 1.21 (3H, t, J = 7.0 Hz, $\underline{CH_3}$–CH_2–O), 2.12 (4H, m, H-3,5), 2.38 (1H, m, H-4), 3.59 (4H, m, H-2,6), 4.16 (2H, q, J = 7.0 Hz, CH_3–$\underline{CH_2}$–O), 7.07 (1H, t, J = 8.5 Hz, H-4'), 7.37 (2H, t, J = 8.5 Hz, H-3',5'), 7.50 (2H, d, J = 8.5 Hz, H-2',6'); ^{13}C NMR (100 MHz, $CDCl_3$): δ 14.1 ($\underline{CH_3}$–CH_2–O), 28.5 (C-3,5), 40.4 (C-4), 46.5 (C-2,6), 61.6 (CH_3–$\underline{CH_2}$–O), 121.6 (C-2',6'), 128.0 (C-4'), 128.9 (C-3',5'), 139.4 (C-1'), 153.3 (C=O), 175.8 (COOEt); HR-EI-MS (*m/z*): 276.1493 $[M]^+$ calculated for $C_{15}H_{20}N_2O_3$; 276.1573.

2.2.2. Synthesis of 1-phenylcarbamoylpiperidine-4-carboxamide (2)

White fluffy precipitates of 1-phenylcarbamoylpiperidine-4-carboxamide (**2**) were obtained when ethyl 1-phenylcarbamoylpiperidine-4-carboxylate (**1**; 0.056 mol, 15.6 g) was stirred for 4–5 h with 50 mL of hydrazine hydrate (80 %) in 100 mL round bottom flask. Precipitates obtained were filtered, washed with cold distilled water, and dried. The physical and spectroscopic data of **2** is as follows:

White shiny powder; Yield: 97 %; M.P.: 163–166 °C; IR (KBr, ν_{max}, cm^{-1}): 3386, 3354 (N–H), 3030 (Ar–H), 2947 (C–H), 1673, 1652 (C=O), 1617–1563 (Ar–C=C), 1239 (C–N); ^{1}H NMR (400 MHz, $CDCl_3$, ppm): δ 2.01 (4H, m, H-3,5), 2.49 (1H, m, H-4), 3.59 (4H, m, H-2,6), 7.07 (1H, t, J = 8.5 Hz, H-4'), 7.30 (2H, J = 8.5 Hz, H-3',5'), 7.58 (2H, d, J = 8.5 Hz, H-2',6'); ^{13}C NMR (100 MHz, $CDCl_3$): δ 29.4 (C-3,5), 40.1 (C-4), 47.0 (C-2,6), 121.6 (C-2',6'), 128.0 (C-4'), 128.9 (C-3',5'), 139.4 (C-1'), 153.5 (C=O), 178.2 (CONH); HR-EI-MS (*m/z*): 262.1449 $[M]^+$ calculated for $C_{13}H_{18}N_4O_2$; 262.1429.

2.2.3. Synthesis of 4-ethyl-(1-phenylcarbamoylpiperidine)thiosemicarbazide (3)

The carboxamide **2** (0.025 mol, 6.5 g) was snapped up in a 50 mL round bottom flask, and an equimolar of ethyl isothiocyanate (0.025 mol, 2.28 mL) was dropped slowly with continuous mixing. The reaction was refluxed and stirred for 3–4 h after adding 30 mL of methanol as a solvent. The precipitates formed on cooling that were filtered, washed, and dried. The physical and spectroscopic data of **3** is as follows:

White powder; Yield: 97 %; M.P.: 180–183 °C; IR (KBr, ν_{max}, cm^{-1}): 3364 (N–H), 3030 (Ar–H), 2916 (C–H), 1669, 1652 (C=O), 1614–1554 (Ar–C=C), 1214 (C–N); ^{1}H NMR (400 MHz, $CDCl_3$, ppm): δ 1.29 (3H, t, J = 7.0 Hz, $\underline{CH_3}$–CH_2–N), 1.89 (4H, m, H-3,5), 2.49 (1H, m, H-4), 3.49 (4H, m, H-2,6), 4.43 (2H, q, J = 7.0 Hz, CH_3–$\underline{CH_2}$–N), 7.07 (1H, t, J = 8.5 Hz, H-4'), 7.37 (2H, J = 8.5 Hz, H-3',5'), 7.50 (2H, d, J = 8.5 Hz, H-2',6'); ^{13}C NMR (100 MHz, $CDCl_3$): δ 15.2 ($\underline{CH_3}$–CH_2–N), 29.4 (C-3,5), 40.0 (CH_3–$\underline{CH_2}$–N), 40.7 (C-4), 47.1 (C-2,6), 121.6 (C-2',6'), 128.0 (C-4'), 128.9 (C-3',5'), 139.4 (C-1'), 153.1 (C=O), 173.2 (CO), 184.2 (C=S); HR-EI-MS (*m/z*): 349.1592 $[M]^+$ calculated for $C_{16}H_{22}N_5O_2S$; 349.1572.

2.2.4. Synthesis of 4-ethyl-5-(1-phenylcarbamoylpiperidine)-4H-1,2,4-triazole-3-thiol (4)

The semicarbazide **3**, obtained in the third step was dissolved in 1 % aqueous NaOH (30 mL) in a 100 mL round bottom flask and refluxed for 4 h. After that, the reaction mixture was transposed into chilled water. Precipitates appeared when acidified to pH 5–6 using dilute HCl, which were filtered, washed, and dried. The physical and spectroscopic data of **4** is as follows:

White powder; Yield: 97 %; M.P.: 210–213 °C; IR (KBr, ν_{max}, cm^{-1}): 3366 (N–H), 3030 (Ar–H), 2930 (C–H), 1661 (C=O), 1616–1549 (Ar–C=C, C=N), 1233 (C–N); ^{1}H NMR (400 MHz, $CDCl_3$, ppm): δ 1.31 (3H, t, J = 7.0 Hz, CH_3–$\underline{CH_2}$–N), 1.89 (4H, m, H-3',5'), 2.83 (1H, m, H-4'), 3.59 (4H, m, H-2',6'), 4.12 (2H, q, J = 7.0 Hz, CH_3–$\underline{CH_2}$–N), 7.07 (1H, t, J = 8.5 Hz, H-4"), 7.37 (2H, J = 8.5 Hz, H-3",5"), 7.50 (2H, d, J = 8.5 Hz, H-2",6"), 13.1 (1H, SH); ^{13}C NMR (100 MHz, $CDCl_3$): δ 14.9 (CH_3), 29.0 (C-3',5'), 31.5 (C-4'), 31.1 (CH_2), 46.7 (C-2',6'), 121.6 (C-2",6"), 128.0 (C-4"), 128.9 (C-3",5"), 139.4 (C-1"), 157.7 (C-5), 156.1 (C=O), 162.3 (C-3); HR-EI-MS (m/z): 331.1486 $[M]^+$ calculated for $C_{16}H_{21}N_5OS$; 331.1466.

2.2.5. General procedure for the synthesis of compounds (6a-n)

The measured amounts of alkyl/aralkyl/aryl amines (**5a-n**, 0.01mol) were taken in quick fit Erlenmeyer flasks (separate for each reaction) containing 20 % aqueous Na_2CO_3 solution (50 mL) to attain the pH 9–10. Then equimolar amount of 2-bromopropionyl bromide was added with constant rigorous shaking till the precipitation occurred. Further stirring the mixture for 1–2 h resulted in homogenous precipitates, which were filtered, washed with cold water, and dried to acquire the particular electrophile(s), *N*-alkyl/aralkyl/aryl substituted-2-bromopropionamides (**6a-n**).

2.2.6. General method for the synthesis of compounds (7a-n)

Compound **4** (0.0006 mol, 0.2 g) was dissolved in ethanolic solution of KOH (0.6 mmol, 0.036 g) and the mixture was stirred for 30 min at RT. The electrophiles (**6a-n,** separately for each analogue) were added and the mixture was refluxed for 4–5 h. The progress of the reaction mixture was monitored by TLC. On completion of the reaction, the excess amount of cold water was added, and the precipitates formed of the targeted products (**7a-n**) were filtered, washed, and dried.

2.2.7. Spectral characterization of the compounds 7a-n

*2.2.7.1. 2-(5-(1-Phenylcarbamoylpiperdine-4-yl)-4-ethyl-4H-1,2,4-triazol-3-ylthio)-N,N-diethylpropanamide (**7a**).* White amorphous powder; Yield: 95 %; M.P.: 98–101 °C; IR (KBr, ν_{max}, cm^{-1}): 3362 (N–H), 3033 (Ar–H), 2932 (C–H), 1682, 1663 (C=O), 1618–1550 (Ar–C=C, C=N), 1258 (C–N); ^{1}H NMR (400 MHz, $CDCl_3$): δ 1.06 (3H, t, J = 7.0 Hz, H-2""), 1.19 (3H, t, J = 7.0 Hz, H-2""'), 1.31 (3H, t, J = 7.0 Hz, $\underline{CH_3}$–CH_2–N), 1.61 (3H, d, J = 7.0 Hz, H-3"'), 1.90–2.05 (4H, m, H-3',5'), 2.82 (1H, m, H-4'), 3.08 (2H, m, H-2',6'), 3.33 (2H, q, J = 7.0 Hz, H-1""), 3.54 (2H, q, J = 7.0 Hz, H-1""'), 3.90 (2H, q, J = 7.0 Hz, CH_3–$\underline{CH_2}$–N), 4.16 (2H, td, J = 7.5, 1.2 Hz, H-2',6'), 4.90 (1H, q, J = 7.0 Hz, H-2"'), 6.70 (1H, s, NH), 7.01 (1H, t, J = 8.0 Hz, H-4"), 7.26 (2H, t, J = 8.0 Hz, H-3",5"), 7.33 (2H, d, J = 8.0, H-2",6"); ^{13}C NMR (100 MHz, $CDCl_3$): δ 12.9 (C-2""), 14.9 (C-2""'), 15.9 ($\underline{CH_3}$–CH_2–N), 19.9 (C-3"'), 30.3 (C-5'), 30.4 (C-3'), 32.8 (C-4'), 38.8 (C-2"'), 41.0 (C-1"'), 42.7 (C-1""'), 43.8 (CH_3–$\underline{CH_2}$–N), 43.9 (C-2'), 44.0 (C-6'), 120.1 (C-2",6"), 123.2 (C-4"), 129.0 (C-3",5"), 139.2 (C-1"), 149.6 (C-3), 155.1 (C=O), 157.4 (C-5), 170.7 (C-1"'); HR-EI-MS (m/z): 458.2483 $[M]^+$ calculated for $C_{23}H_{34}N_6O_2S$; 458.2463.

*2.2.7.2. 2-(5-(1-Phenylcarbamoylpiperdine-4-yl)-4-ethyl-4H-1,2,4-triazol-3-ylthio)-N-cyclohexylpropanamide (**7b**).* White amorphous powder; Yield 95 %; M.P.: 142–145 °C; IR (KBr, ν_{max}, cm^{-1}): 3361 (N–H), 3034 (Ar–H), 2933 (C–H), 1681, 1663 (C=O), 1617–1550 (Ar–C=C, C=N), 1259 (C–N); ^{1}H NMR (400 MHz, $CDCl_3$): δ 1.14–1.27 (6H, m, H-3""-5""), 1.33 (3H, t, J = 7.3 Hz, $\underline{CH_3}$–CH_2–N), 1.53 (3H, d, J = 7.3 Hz, H-3"'), 1.62–1.67 (2H, m, H-2"",6""), 1.80–1.84 (2H, m, H-2"",6""), 1.95–2.05 (4H, m, H-3',5'), 2.83 (1H, m, H-4'), 3.08 (2H, m, H-2',6'), 3.68 (1H, m, H-1""), 3.89 (2H, q, J = 7.3 Hz, CH_3–$\underline{CH_2}$–N), 4.18 (2H, m, H-2',6'), 4.25 (1H, q, J = 7.3 Hz, H-2"'), 7.02 (1H, t, J = 8.3 Hz, H-4"), 7.26 (2H, t, J = 8.3 Hz, H-3",5"), 7.33 (2H, d, J = 8.3 Hz, H-2",6"); ^{13}C NMR (100 MHz, $CDCl_3$): δ 15.8 ($\underline{CH_3}$–CH_2–N), 16.9 (C-3"'), 24.6 (C-3""), 25.5 (C-5""), 30.3 (C-4""), 30.3 (C-2""), 30.4 (C-6""), 31.7 (C-3'), 32.3 (C-5'), 32.7 (C-4'), 38.9 (C-2"'), 44.1 (C-2'), 44.4 (C-6'), 44.9 (CH_3–$\underline{CH_2}$–N), 48.4 (C-1""), 120.2 (C-2",6"), 123.3 (C-4"), 128.9 (C-3",5"), 139.1 (C-1"), 150.3 (C-3), 155.1 (C=O), 157.4 (C-5), 170.2 (C-1"'); HR-EI-MS (m/z): 484.2640 $[M]^+$ calculated for $C_{25}H_{36}N_6O_2S$; 484.2620.

*2.2.7.3. 2-(5-(1-Phenylcarbamoylpiperdine-4-yl)-4-ethyl-4H-1,2,4-triazol-3-ylthio)-N-benzylpropanamide (**7c**).* White amorphous powder; Yield 94 %; M.P.: 107–109 °C; IR (KBr, ν_{max}, cm^{-1}): 3363 (N–H), 3032 (Ar–H), 2931 (C–H), 1683, 1664 (C=O), 1619–1551 (Ar–C=C, C=N), 1259 (C–N); ^{1}H NMR (400 MHz, $CDCl_3$): δ 1.31 (3H, t, J = 7.3 Hz, $\underline{CH_3}$–CH_2–N), 1.60 (3H, d, J = 7.3 Hz, H-3"'), 1.90–2.01 (4H, m, H-3',5'), 2.80 (1H, m, H-4'), 3.09 (2H, q, J = 7.3 Hz, CH_3–$\underline{CH_2}$–N), 3.85 (2H, m, H-2',6'), 4.15 (1H, td, J = 7.5, 1.2 Hz, H-2',6'), 4.40 (3H, m, signal overlapped, H-2"',7""), 7.04 (1H, t, J = 7.3 Hz, H-4"), 7.22 (3H, m, H-2""-4""), 7.25 (2H, m, H-5"",6""), 7.28 (2H, t, J = 8.3 Hz, H-3",5"), 7.34 (2H, d, J = 8.5 Hz, H-2",6"); ^{13}C NMR (100 MHz, $CDCl_3$): δ 15.7 ($\underline{CH_3}$–CH_2–N), 16.9 (C-3"'), 30.2 (C-3'), 30.3 (C-5'), 32.6 (C-4'), 38.9 (C-2"'), 43.6 (C-7""), 43.6 (CH_3–$\underline{CH_2}$–N), 43.7 (C-6'), 43.9 (C-2'), 120.1 (C-2",6"), 123.3 (C-4"), 127.2 (C-4""), 127.6 (C-3"",5""), 128.5 (C-2"",6""), 129.0 (C-1""), 129.0 (C-3",5"), 138.5 (C-3), 139.0 (C-1"), 155.1 (C=O), 157.4 (C-5), 171.4 (C-1"'); HR-EI-MS (m/z): 492.2327 $[M]^+$ calculated for $C_{26}H_{32}N_6O_2S$; 492.2307.

*2.2.7.4. 2-(5-(1-Phenylcarbamoylpiperdine-4-yl)-4-ethyl-4H-1,2,4-triazol-3-ylthio)-N-2-methylphenylpropanamide (**7d**).* White amorphous powder; Yield: 94 %; M.P.: 163–165 °C; IR (KBr, ν_{max}, cm^{-1}): 3361 (N–H), 3032 (Ar–H), 2933 (C–H), 1683, 1664 (C=O), 1617–1549 (Ar–C=C, C=N), 1257 (C–N); ^{1}H NMR (400 MHz, $CDCl_3$): δ 1.34 (3H, t, J = 7.0 Hz, $\underline{CH_3}$–CH_2–N), 1.66 (3H, d, J = 7.0 Hz, H-3"'), 1.89–2.06 (4H, m, H-3',5'), 2.20 (3H, s, CH_3), 2.84 (1H, m, H-4'), 3.07 (2H, m, H-2,'6'), 3.84 (2H, q, J = 7.0 Hz, CH_3–$\underline{CH_2}$–N), 4.16 (2H, m, H-2',6'), 4.63 (1H, q, J = 7.0 Hz, H-2"'), 6.90–7.03 (2H, m, H-5"",6""), 7.11–7.14 (2H, m, H-3"",4""), 7.16 (1H, t, J = 8.0 Hz, H-4"), 7.29 (2H, t, J = 8.0 Hz, H-3",5"), 7.36 (2H, d, J = 8.0 Hz, H-2",6"); ^{13}C NMR (100 MHz, $CDCl_3$): δ 15.6 ($\underline{CH_3}$–CH_2–N), 16.6 (C-3"'), 18.3 (CH_3), 30.3 (C-5'), 30.4 (C-3'), 32.7 (C-4'), 38.9 (C-2"'), 43.6 (CH_3–$\underline{CH_2}$–N), 43.9 (C-2'), 44.0 (C-6'), 120.1 (C-2",6"), 122.4 (C-6""), 123.3 (C-3""), 124.8 (C-4"), 129 (C-3",5"), 129.3 (C-5""), 130.5 (C-2""), 136.4 (C-1""), 150.9 (C-3), 155.1 (C=O), 157.9 (C-5),

169.7 (C-1'''); HR-EI-MS (*m/z*): 492.2327 $[M]^+$ calculated for $C_{26}H_{32}N_6O_2S$; 492.2307.

*2.2.7.5. 2-(5-(1-Phenylcarbamoylpiperdine-4-yl)-4-ethyl-4H-1,2,4-triazol-3-ylthio)-N-3-methylphenylpropanamide (**7e**).* White amorphous powder; Yield: 94 %; M.P.: 100–103 °C; IR (KBr, ν_{max}, cm^{-1}): 3363 (N–H), 3031 (Ar–H), 2933 (C–H), 1681, 1663 (C=O), 1616–1551 (Ar–C=C, C=N), 1259 (C–N); ^{1}H NMR (400 MHz, $CDCl_3$): δ 1.33 (3H, t, J = 7.3 Hz, $\underline{CH_3}$–CH_2–N), 1.64 (3H, d, J = 7.3 Hz, H-3'''), 1.90–2.06 (4H, m, H-3',5'), 2.29 (3H, s, CH_3), 2.82 (1H, m, H-4'), 3.06 (2H, m, H-2',6'), 3.86 (2H, q, J = 7.3 Hz, CH_3–$\underline{CH_2}$–N), 4.16 (2H, m, H-2',6'), 4.48 (1H, q, J = 7.3 Hz, H-2'''), 6.85 (1H, d, J = 8.5 Hz, H-6''''), 7.02 (1H, t, J = 8.3 Hz, H-4''), 7.14 (1H, t, J = 8.8 Hz, H-5''''), 7.27 (2H, t, J = 8.3 Hz, H-3'',5''), 7.33 (1H, s, H-2''''), 7.35 (2H, d, J = 8.3 Hz, H-2'',6''), 7.38 (1H, d, J = 8.8 Hz, H-4''''); ^{13}C NMR (100 MHz, $CDCl_3$): δ 15.7 ($\underline{CH_3}$–CH_2–N), 16.5 (CH_3), 21.6 (C-3'''), 30.3 (C-5'), 30.4 (C-3'), 32.8 (C-4'), 39.0 (C-2'''), 44.0 (C-2',6'), 44.4 (CH_3–$\underline{CH_2}$–N), 116.9 (C-2''''), 120.2 (C-2'',6''), 120.3 (C-6''''), 123.3 (C-4''), 124.9 (C-4''''), 128.8 (C-5''''), 129.0 (C-3'',5''), 138.4 (C-3''''), 138.9 (C-1''''), 139.0 (C-1''), 150.1 (C-3), 155.1 (C=O), 157.6 (C-5), 169.3 (C-1'''); HR-EI-MS (*m/z*): 492.2327 $[M]^+$ calculated for $C_{26}H_{32}N_6O_2S$; 492.2307.

*2.2.7.6. 2-(5-(1-Phenylcarbamoylpiperdine-4-yl)-4-ethyl-4H-1,2,4-triazol-3-ylthio)-N-2-ethylphenylpropanamide (**7f**).* White amorphous powder; Yield: 97 %; M.P.: 179–180 °C; IR (KBr, ν_{max}, cm^{-1}): 3361 (N–H), 3032 (Ar–H), 2931 (C–H), 1683, 1664 (C=O), 1618–1552 (Ar–C=C, C=N), 1259 (C–N); ^{1}H NMR (400 MHz, $CDCl_3$): δ 1.08 (3H, t, J = 7.5 Hz, $\underline{CH_3}$–CH_2), 1.35 (3H, t, J = 7.3 Hz, $\underline{CH_3}$–CH_2–N), 1.67 (3H, d, J = 7.3 Hz, H-3'''), 1.91–2.05 (4H, m, H-3',5'), 2.55 (2H, q, J = 7.5 Hz, CH_3–$\underline{CH_2}$), 2.83 (1H, m, H-4'), 3.08 (2H, m, H-2',6'), 3.87 (2H, q, J = 7.3 Hz, CH_3–$\underline{CH_2}$–N), 4.17 (2H, m, H-2',6'), 4.61 (1H, q, J = 7.3 Hz, H-2'''), 7.03 (1H, t, J = 8.0 Hz, H-4''), 7.06 (1H, d, J = 8.0 Hz, H-6''''), 7.17 (1H, t, J = 8.0 Hz, H-4''''), 7.26 (2H, t, J = 8.0 Hz, H-3'',5''), 7.27 (1H, t, J = 8.0 Hz, H-5''''), 7.35 (2H, d, J = 8.0 Hz, H-2'',6''), 7.84 (1H, d, J = 8.0 Hz, H-3''''); ^{13}C NMR (100 MHz, $CDCl_3$): δ 14.3 (CH_3), 15.6 ($\underline{CH_3}$–CH_2–N), 16.7 (C-3'''), 24.6 (CH_2), 30.3 (C-5'), 30.4 (C-3'), 32.7 (C-4'), 38.9 (C-2'''), 43.5 (CH_3–$\underline{CH_2}$–N), 43.9 (C-2'), 44.0 (C-6'), 120.1 (C-2'',6''), 123.3 (C-4''), 123.5 (C-4''''), 125.3 (C-6''''), 126.4 (C-3''''), 128.8 (C-5''''), 129.0 (C-3'',5''), 135.5 (C-2''''), 135.7 (C-1''''), 139.0 (C-1''), 151.0 (C-3), 155.0 (C=O), 157.7 (C-5), 169.8 (C-1'''); HR-EI-MS (*m/z*): 506.2483 $[M]^+$ calculated for $C_{27}H_{34}N_6O_2S$; 506.2463.

*2.2.7.7. 2-(5-(1-Phenylcarbamoylpiperdine-4-yl)-4-ethyl-4H-1,2,4-triazol-3-ylthio)-N-4-ethylphenylpropanamide (**7g**).* White amorphous powder; Yield: 95 %; M.P.: 106–108 °C; IR (KBr, ν_{max}, cm^{-1}): 3363 (N–H), 3034 (Ar–H), 2933 (C–H), 1683, 1664 (C=O), 1617–1551 (Ar–C=C, C=N), 1256 (C–N); ^{1}H NMR (400 MHz, $CDCl_3$): δ 1.17 (3H, t, J = 7.6 Hz, $\underline{CH_3}$–CH_2), 1.33 (3H, t, J = 7.3 Hz, $\underline{CH_3}$–CH_2–N), 1.64 (3H, d, J = 7.3 Hz, H-3'''), 1.90–2.06 (4H, m, H-3',5'), 2.57 (2H, q, J = 7.6 Hz, CH_3–$\underline{CH_2}$), 2.84 (1H, m, H-4'), 3.07 (2H, m, H-2,'6'), 3.89 (2H, q, J = 7.3 Hz, CH_3–$\underline{CH_2}$–N), 4.19 (2H, m, H-2',6'), 4.48 (1H, q, J = 7.3 Hz, H-2'''), 7.02 (1H, t, J = 8.5 Hz, H-4''), 7.08 (2H, d, J = 8.5 Hz, H-2'''',6''''), 7.25 (2H, d, J = 8.5 Hz, H-3'''',5''''), 7.27 (2H, t, J = 8.5 Hz, H-3'',5''), 7.34 (2H, d, J = 8.5 Hz, H-2'',6''); ^{13}C NMR (100 MHz, $CDCl_3$): δ 15.7 (CH_3), 15.9 ($\underline{CH_3}$–CH_2–N), 16.5 (C-3'''), 28.4 (CH_2), 30.3 (C-5'), 30.4 (C-3'), 32.8 (C-4'), 39.0 (C-2'''), 44.0 (CH_3–$\underline{CH_2}$–N), 44.1 (C-2'), 44.2 (C-6'), 119.8 (C-2'''',6''''), 120.1 (C-2'',6''), 123.3 (C-4''), 128.3 (C-3'''',5''''), 129.0 (C-3'',5''), 136.2 (C-4''''), 139.0 (C-1''), 140.2 (C-1''''), 150.9 (C-3), 155.0 (C=O), 157.6 (C-5), 169.1 (C-1'''); HR-EI-MS (*m/z*): 506.2483 $[M]^+$ calculated for $C_{27}H_{34}N_6O_2S$; 506.2463.

*2.2.7.8. 2-(5-(1-Phenylcarbamoylpiperdine-4-yl)-4-ethyl-4H-1,2,4-triazol-3-ylthio)-N-2,3-dimethylphenylpropanamide (**7h**).* White amorphous powder; Yield 90 %; M.P.: 142–145 °C; IR (KBr, ν_{max}, cm^{-1}): 3361 (N–H), 3032 (Ar–H), 2931 (C–H), 1681, 1662 (C=O), 1618–1551 (Ar–C=C, C=N), 1258 (C–N); ^{1}H NMR (400 MHz, $CDCl_3$): δ 1.34 (3H, t, J = 7.3 Hz, $\underline{CH_3}$–CH_2–N), 1.65 (3H, d, J = 7.3 Hz, H-3'''), 1.90–2.04 (4H, m, H-3',5'), 2.11 (3H, s, CH_3), 2.24 (3H, s, CH_3), 2.84 (1H, m, H-4'), 3.07 (2H, m, H-2',6'), 3.89 (2H, q, J = 7.3 Hz, CH_3–$\underline{CH_2}$–N), 4.15 (2H, m, H-2',6'), 4.61 (1H, q, J = 7.3 Hz, H-2'''), 6.94 (1H, d, J = 8.5 Hz, H-4''''), 7.01 (1H, t, J = 8.5 Hz, H-4''), 7.05 (1H, t, J = 8.5 Hz, H-5''''), 7.27 (2H, t, J = 8.5 Hz, H-3'',5''), 7.34 (2H, d, J = 8.5 Hz, H-2'',6''), 7.74 (1H, d, J = 8.5 Hz, H-6''''); ^{13}C NMR (100 MHz, $CDCl_3$): δ 13.9 (CH_3), 15.6 (CH_3), 16.7 ($\underline{CH_3}$–CH_2–N), 20.7 (C-3'''), 30.3 (C-3'), 30.4 (C-5'), 32.7 (C-4'), 39.0 (C-2'''), 43.8 (CH_3–$\underline{CH_2}$–N), 43.8 (C-6'), 44.0 (C-2'), 120.1 (C-2'',6''), 121.4 (C-4''''), 123.3 (C-4''), 125.7 (C-5''''), 126.9 (C-6''''), 129.0 (C-3'',5''), 129.2 (C-3''''), 136.0 (C-2''''), 137.3 (C-1''''), 139.0 (C-1''), 150.9 (C-3), 155.0 (C=O), 157.6 (C-5), 169.8 (C-1'''); HR-EI-MS (*m/z*): 506.2483 $[M]^+$ calculated for $C_{27}H_{34}N_6O_2S$; 506.2463.

*2.2.7.9. 2-(5-(1-Phenylcarbamoylpiperdine-4-yl)-4-ethyl-4H-1,2,4-triazol-3-ylthio)-N-2,4-dimethylphenylpropanamide (**7i**).* White amorphous powder; Yield: 96 %; M.P.: 190–193 °C; IR (KBr, ν_{max}, cm^{-1}): 3362 (N–H), 3033 (Ar–H), 2932 (C–H), 1682, 1663 (C=O), 1618–1550 (Ar–C=C, C=N), 1258 (C–N); ^{1}H NMR (400 MHz, $CDCl_3$): δ 1.34 (3H, t, J = 7.3 Hz, $\underline{CH_3}$–CH_2–N), 1.65 (3H, d, J = 7.3 Hz, H-3'''), 1.89–2.03 (4H, m, H-3',5'), 2.18 (3H, s, CH_3), 2.24 (3H, s, CH_3), 2.83 (1H, m, H-4'), 3.08 (2H, m, H-2',6'), 3.89 (2H, q, J = 7.3 Hz, CH_3–$\underline{CH_2}$–N), 4.15 (2H, m, H-2',6'), 4.61 (1H, q, J = 7.3 Hz, H-2'''), 7.03 (1H, t, J = 8.5 Hz, H-4''), 7.25 (1H, s, H-3''''), 7.28 (2H, t, J = 8.5 Hz, H-3'',5''), 7.29 (1H, d, J = 8.2 Hz, H-6''''), 7.32 (1H, d, J = 8.2 Hz, H-5''''), 7.34 (2H, d, J = 8.5 Hz, H-2'',6''); ^{13}C NMR (100 MHz, $CDCl_3$): δ 15.6 ($\underline{CH_3}$–CH_2–N), 16.7 (C-3'''), 18.2 (CH_3), 20.9 (CH_3), 30.3 (C-5'), 30.4 (C-3'), 32.7 (C-4'), 38.9 (C-2'''), 43.7 (CH_3–$\underline{CH_2}$–N), 43.9 (C-6'), 44.0 (C-2'), 120.1 (C-2'',6''), 122.6 (C-6''''), 123.3 (C-4''), 127.0 (C-3''''), 129.0 (C-3'',5''), 129.5 (C-5''''), 131.2 (C-4''''), 133.7 (C-2''''), 134.5 (C-1''''), 139.0 (C-1''), 150.9 (C-3), 155.0 (C=O), 157.7 (C-5), 169.6 (C-1'''); HR-EI-MS (*m/z*): 506.2483 $[M]^+$ calculated for $C_{27}H_{34}N_6O_2S$; 506.2463.

*2.2.7.10. 2-(5-(1-Phenylcarbamoylpiperdine-4-yl)-4-ethyl-4H-1,2,4-triazol-3-ylthio)-N-2,5-dimethylphenylpropanamide (**7j**).* White amorphous powder; Yield: 93 %; M.P.: 167–170 °C; IR (KBr, ν_{max}, cm^{-1}): 3362 (N–H), 3034 (Ar–H), 2932 (C–H), 1683, 1664 (C=O), 1618–1553 (Ar–C=C, C=N), 1259 (C–N); ^{1}H NMR (400 MHz, $CDCl_3$): δ 1.34 (3H, t, J = 7.3 Hz, $\underline{CH_3}$–CH_2–N), 1.66 (3H, d, J = 7.3 Hz,

H-3'''), 1.89–2.06 (4H, m, H-3',5'), 2.14 (3H, s, CH_3), 2.27 (3H, s, CH_3), 2.82 (1H, m, H-4'), 3.10 (2H, m, H-2',6'), 3.83 (2H, q, $J = 7.3$ Hz, CH_3–$\underline{CH_2}$–N), 4.15 (2H, m, H-2',6'), 4.62 (1H, q, $J = 7.3$ Hz, H-2'''), 6.82 (1H, d, $J = 8.5$ Hz, H-4'''), 6.99 (1H, d, $J = 8.5$ Hz, H-3'''), 7.03 (1H, t, $J = 8.5$ Hz, H-4''), 7.25 (1H, s, H-6'''), 7.28 (2H, t, $J = 8.5$ Hz, H-3",5"), 7.34 (2H, d, $J = 8.5$ Hz, H-2",6"); ^{13}C NMR (100 MHz, $CDCl_3$): δ 15.5 ($\underline{CH_3}$–CH_2–N), 16.6 (C-3'''), 17.8 (CH_3), 21.2 (CH_3), 30.3 (C-5'), 30.4 (C-3'), 32.6 (C-4'), 38.9 (C-2'''), 43.9 (CH_3–$\underline{CH_2}$–N), 44.0 (C-2'), 120.1 (C-2",6"), 123.0 (C-4'''), 123.2 (C-4''), 123.5 (C-6'''), 126.1 (C-3'''), 129.0 (C-3",5"), 130.3 (C-2'''), 136.1 (C-5''), 136.2 (C-1'''), 139.0 (C-1''), 150.9 (C-3), 155.0 (C=O), 157.5 (C-5), 169.6 (C-1'''); HR-EI-MS (m/z): 506.2483 $[M]^+$ calculated for $C_{27}H_{34}N_6O_2S$; 506.2463.

2.2.7.11. 2-(5-(1-Phenylcarbamoylpiperdine-4-yl)-4-ethyl-4H-1,2,4-triazol-3-ylthio)-N-2,6-dimethylphenylpropanamide ***(7k)***. White amorphous powder; Yield: 83 %; M.P.: 188–190 °C; IR (KBr, ν_{max}, cm^{-1}): 3361 (N–H), 3032 (Ar–H), 2931 (C–H), 1681, 1662 (C=O), 1618–1549 (Ar–C=C, C=N), 1258 (C–N); ^{1}H NMR (400 MHz, $CDCl_3$+CD_3OD): δ 1.36 (3H, t, $J = 7.2$ Hz, $\underline{CH_3}$–CH_2–N), 1.69 (3H, d, $J = 7.2$ Hz, H-3'''), 1.90–2.00 (4H, m, H-3',5'), 2.11 (6H, s, 2 × CH_3), 2.99 (1H, m, H-4'), 3.07 (2H, m, H-2',6'), 3.40 (2H, q, $J = 7.2$ Hz, CH_3–$\underline{CH_2}$–N), 4.16 (2H, m, H-2',6'), 4.68 (1H, q, $J = 7.2$ Hz, H-2'''), 6.67–6.99 (3H, m, H-3'''-5'''), 7.02 (1H, t, $J = 8.6$ Hz, H-4''), 7.29 (2H, t, $J = 8.6$ Hz, H-3",5"), 7.37 (2H, d, $J = 8.6$ Hz, H-2",6"); ^{13}C NMR (100 MHz, $CDCl_3$+CD_3OD): δ 15.3 ($\underline{CH_3}$–CH_2–N), 15.6 (C-3'''), 18.2 (CH_3), 20.9 (CH_3), 29.1 (C-3''), 29.1 (C-5'), 31.6 (C-4'), 37.4 (CH_3–$\underline{CH_2}$–N), 37.7 (C-2'''), 42.6 (C-6'), 44.3 (C-2'), 119.5 (C-2",6"), 121.9 (C-4''), 128.1 (C-5'''), 128.1 (C-3'''), 128.6 (C-3",5"), 131.0 (C-4'''), 132.8 (C-6'''), 132.9 (C-2'''), 134.0 (C-1'''), 138.0 (C-1''), 148.4 (C-3), 155.0 (C=O), 157,0 (C-5), 169.3 (C-1'''); HR-EI-MS (m/z): 506.2483 $[M]^+$ calculated for $C_{26}H_{32}N_6O_2S$; 506.2463.

2.2.7.12. 2-(5-(1-Phenylcarbamoylpiperdine-4-yl)-4-ethyl-4H-1,2,4-triazol-3-ylthio)-N-3,4-dimethylphenylpropanamide ***(7l)***. White amorphous powder; Yield: 85 %; M.P.: 180–183 °C; IR (KBr, ν_{max}, cm^{-1}): 3356 (N–H), 3036 (Ar–H), 2944 (C–H), 1686, 1663 (C=O), 1618–1551 (Ar–C=C, C=N), 1267 (C–N); ^{1}H NMR (400 MHz, $CDCl_3$): δ 1.32 (3H, t, $J = 7.3$ Hz, $\underline{CH_3}$–CH_2–N), 1.63 (3H, d, $J = 7.3$ Hz, H-3'''), 1.89–2.08 (4H, m, H-3',5'), 2.17 (3H, s, CH_3), 2.19 (3H, s, CH_3), 2.83 (1H, m, H-4'), 3.08 (2H, m, H-2',6'), 3.88 (2H, q, $J = 7.3$ Hz, CH_3–$\underline{CH_2}$–N), 4.47 (1H, q, $J = 7.3$ Hz, H-2'''), 4.16 (2H, m, H-2',6'), 6.70 (1H, s, H-2'''), 7.03 (1H, t, $J = 8.6$ Hz, H-4''), 7.04 (1H, d, $J = 8.5$ Hz, H-6'''), 7.28 (2H, t, $J = 8.6$ Hz, H-3",5"), 7.29 (1H, d, $J = 8.5$ Hz, H-5'''), 7.32 (2H, d, $J = 8.6$ Hz, H-2",6") 7.33 (1H, d, $J = 8.5$ Hz, H-6'''); ^{13}C NMR (100 MHz, $CDCl_3$): δ 15.6 ($\underline{CH_3}$–CH_2–N), 16.5 (C-3'''), 19.2 (CH_3), 19.9 (CH_3), 30.2 (C-5'), 30.3 (C-3'), 32.8 (C-4'), 39.0 (C-2'''), 43.9 (CH_3–$\underline{CH_2}$–N), 44.0 (C-6'), 44.4 (C-2'), 117.5 (C-2'''), 117.5 (C-6'''), 120.1 (C-2",6"), 123.3 (C-4''), 125.9 (C-5'''), 129.0 (C-3",5"), 138.2 (C-1'''), 138.6 (C-3'''), 138.6 (C-4'''), 139.0 (C-1''), 150.1 (C-3), 155.0 (C=O), 157.6 (C-5), 169.2 (C-1'''); HR-EI-MS (m/z): 506.2483 $[M]^+$ calculated for $C_{22}H_{32}N_6O_2S$; 506.2463.

2.2.7.13. 2-(5-(1-Phenylcarbamoylpiperdine-4-yl)-4-ethyl-4H-1,2,4-triazol-3-ylthio)-N-3,5-dimethylphenylpropanamide ***(7m)***. White amorphous powder; Yield: 96 %; M.P.: 196–199 °C; IR (KBr, ν_{max}, cm^{-1}): 3353 (N–H), 3035 (Ar–H), 2950 (C–H), 1680, 1661 (C=O), 1616–1552 (Ar–C=C, C=N), 1268 (C–N); ^{1}H NMR (400 MHz, $CDCl_3$): δ 1.33 (3H, t, $J = 7.3$ Hz, $\underline{CH_3}$–CH_2–N), 1.63 (3H, d, $J = 7.3$ Hz, H-3'''), 1.91–2.06 (4H, m, H-3',5'), 2.25 (6H, s, CH_3), 2.83 (1H, m, H-4'), 3.06 (2H, m, H-2,'6'), 3.87 (2H, q, $J = 7.3$ Hz, CH_3–$\underline{CH_2}$–N), 4.48 (1H, q, $J = 7.3$ Hz, H-2'''), 4.16 (2H, m, H-2',6'), 6.70 (1H, s, H-4'''), 7.03 (1H, t, $J = 8.5$ Hz, H-4''), 7.23 (1H, s, H-2'''), 7.25 (1H, s, H-6'''), 7.28 (2H, t, $J = 8.5$ Hz, H-3",5"), 7.34 (2H, d, $J = 8.5$ Hz, H-2",6"); ^{13}C NMR (100 MHz, $CDCl_3$): δ 15.6 ($\underline{CH_3}$–CH_2–N), 16.5 (C-3'''), 21.5 (2 × CH_3), 30.2 (C-5'), 30.3 (C-3'), 32.8 (C-4'), 39.0 (C-2'''), 43.9 (CH_3–$\underline{CH_2}$–N), 44.0 (C-6'), 44.4 (C-2'), 117.5 (C-2'''), 117.5 (C-6'''), 120.1 (C-2",6"), 123.3 (C-4''), 125.9 (C-4'''), 129.0 (C-3",5"), 138.2 (C-1'''), 138.6 (C-3'''), 138.6 (C-5'''), 139.0 (C-1''), 150.1 (C-3), 155.0 (C=O), 157.6 (C-5), 169.2 (C-1'''); HR-EI-MS (m/z): 506.2483 $[M]^+$ calculated for $C_{27}H_{34}N_6O_2S$; 506.2307.

2.2.7.14. 2-(5-(1-Phenylcarbamoylpiperdine-4-yl)-4-ethyl-4H-1,2,4-triazol-3-ylthio)-N-phenylpropanamide ***(7n)***. White amorphous powder; Yield: 94 %; M.P.: 131–133 °C; IR (KBr, ν_{max}, cm^{-1}): 3354 (N–H), 3040 (Ar–H), 2953 (C–H), 1682, 1663 (C=O), 1614–1550 (Ar–C=C, C=N), 1265 (C–N); ^{1}H NMR (400 MHz, $CDCl_3$): 1.33 (3H, t, $J = 7.3$ Hz, $\underline{CH_3}$–CH_2–N), 1.64 (3H, d, $J = 7.3$ Hz, H-3'''), 1.89–2.08 (4H, m, H-3',5'), 2.82 (1H, m, H-4'), 3.11 (2H, m, H-2',6'), 3.88 (2H, q, $J = 7.3$ Hz, CH_3–$\underline{CH_2}$–N), 4.16 (2H, m, H-2',6'), 4.50 (1H, q, $J = 7.3$ Hz, H-2'''), 7.04 (1H, q, $J = 8.5$ Hz, H-4''), 7.25 (1H, t, $J = 8.5$ Hz, H-4'''), 7.26 (1H, t, $J = 8.5$ Hz, H-3'''), 7.29 (1H, t, $J = 8.5$ Hz, H-5'''), 7.29 (2H, t, $J = 8.5$ Hz, H-3",5"), 7.35 (2H, d, $J = 8.5$ Hz, H-2",6"), 7.59 (1H, d, $J = 8.5$ Hz, H-2'''), 7.60 (1H, d, $J = 8.5$ Hz, H-6'''); ^{13}C NMR (100 MHz, $CDCl_3$): δ 15.6 ($\underline{CH_3}$–CH_2–N), 16.5 (C-3'''), 30.2 (C-5'), 30.3 (C-3'), 32.8 (C-4'), 39.0 (C-2'''), 43.9 (CH_3–$\underline{CH_2}$–N), 44.0 (C-6'), 44.4 (C-2'), 117.5 (C-2''',6'''), 120.1 (C-2",6"), 123.3 (C-4''), 125.9 (C-4'''), 129.0 (C-3",5"), 138.2 (C-1'''), 138.6 (C-3''',5'''), 139.0 (C-1''), 150.1 (C-3), 155.0 (C=O), 157.6 (C-5), 169.2 (C-1'''); HR-EI-MS (m/z): 478.2170 $[M]^+$ calculated for $C_{22}H_{32}N_6O_2S$; 478.2150.

2.3. 15-LOX inhibition assay

The 15-LOX inhibition assay was carried out using chemiluminescence method as described ealier [56]. Briefly, a overall volume of 100 μL reaction mixture in a black 96-well plate contained 60 μL of 200 mM borate buffer pH 9.0, 10 μL of test solution and 10 μL soybean 15-LOX solution. The reaction material was mixed and pre-incubated at 25 °C in the dark for 5 min. Ten μL of 3 nM luminol comprising 1 nM cytochrome *c* solution was added in the reaction well. Ten μL of the substrate linoleic acid solution was added to initiate the reaction. The relative counts were measured from 100 to 300 s of the start of reaction by Synergy HTX BioTek USA plate reader. All experiments were performed in triplicates with negative and positive controls. The active test solutions were suitably diluted and assayed to determine their percentage inhibitions and data was used for the determination of IC_{50} values [56,57].

2.4. Cell viability assay

Cell viability assays were performed using MTT method optimized using human blood mononuclear cells (MNCs) as reported [56, 57]. Briefly, MNCs were isolated using density gradient Lymphocyte Separation Medium of density 1.077 g/mL. MNCs collected at the interface were washed 50 mM phosphate buffer saline (PBS), pH 7.4 and stored in the concentration of 20,000 to 30,00 cells per 10 μL volume. The assay contents contained known volume of PBS, 20 μL test solution and 10 μL MNCs in the 96 well plate and were incubated for 2 h at 37 °C. After given time, 10 μL of 5 mg/mL solution of MTT (3-(4,5-dimethylthiazol-2-yl)-2,5-diphenyltetrazoliumbromide) tetrazolium) was added. The plate was incubated for 18–20 h at 37 °C. Next day, 100 μL DMSO was added to make the total volume of 200 μL. The incubation was continued for further 2 h and absorbance measured at 540 nm. All test solutions along with both positive and negative controls were used in triplicates and data was expressed as Mean ± SEM, n = 3.

2.5. ADME studies

The pharmacodynamic properties (ADME: absorption, distribution, metabolism, excretion) of the compounds **7a-n** were calculated using *MedChem Designer software version 3.0.*

2.6. Computational studies

2.6.1. Molecular docking

Molecular Operating Environment (MOE, version 2015.10) system was used for molecular docking studies [58–60]. Protein was downloaded from PDB (ID: 3PZW) and prepared for docking using the standard procedure. Desired features of protein were generated first, forcefield MMFF94x loaded and heteroatoms and water molecules were removed. Polar hydrogen and charges were incorporated. The database of ligands was created. Dummies on amino acids of the active pocket were built and the ligands were docked with the prepared receptor protein. Over ten poses were set for docking. Docking poses with minimum binding free energy and RMSD value ≤ 2 were selected and visualized for the interactions of ligand and the receptor.

2.6.2. DFT calculations

Density functional theory (DFT) calculations were used to calculate the optimized geometry of the said molecules. DFT data demonstrates the ability of chemical reactivity and stability of a compound. These investigations were carried out using Gaussian 09W software with the basis set of STO-3G [60–62]. The file was visualized in Gauss View 6.0.

3. Results and discussion

3.1. Chemistry

The endeavor of our research was to synthesize 14 new *N*-alkyl/aralkyl/aryl triazole derivatives (**7a-n**) with various substituents and to appraise them for their *in vitro* enzyme inhibition screening against 15-LOX supported by *in silico* studies. Synthesis of intermediates as well as the target compounds was ascertained by the procedure as shown in Scheme 1. The synthesis was started by mixing/rubbing phenylisocyanate with isonipecotate (**a**) which on further treatment with hydrazine hydrate resulted in N-substituted ester (**1**) first and then hydrazide (**2**), respectively. The ^{1}H NMR spectrum of **2** sported two singlets at δ 4.04 (1H, NH) and 8.90 (2H, NH_2) that prove the presence of $NHNH_2$ group. The hydrazide (**2**), refluxed with ethyl isothiocyanate, yielded *N*-ethyl-(1-phenylcarbamoylpiperidine)thiosemicarbazide (**3**). To obtain intramolecular cyclized product 4-ethyl-5-(1-phenylcarbamoylpiperidine)-4H-1,2,4-triazole-3-thiol (**4**), the thiosemicarboxamide **3** was refluxed in alkaline conditions (10 % NaOH). The *N*-alkyl/aralkyl/aryl of 2-bromopropanamides (**6a-n**), the subsequent entities of target compounds were achieved by stirring alkyl/aralkyl/aryl amines (**5a-n**; Table 1) with 2-bromopropionyl bromide in an alkaline solution (pH 9–10). The culminating step was the reaction of compound **4**, separately with each of the electrophile (**6a-n**), separately, to acquire the target compounds **7a-n**, respectively. This chore was achieved according to the protocol as detailed in the experimental part.

The compound **7a** was obtained as a white amorphous powder. The infrared (IR) spectrum showed the absorption bands at 3262, 3033, 2932, 1682, 1663, 1618–1550, 1258 cm^{-1} for N–H, Ar–H, C–H, C=O, Ar–C=C, C=N and, C–N functionalities, respectively. Resonance due to three N-ethyl moieties in the ^{1}H NMR spectrum of **7a** was found at δ 1.05 (3H, t, J = 7.0 Hz, H-2""), 1.18 (3H, t, J = 7.0 Hz, H-2""), 1.32 (3H, t, J = 7.0 Hz, $\underline{CH_3}$–CH_2–N), and 3.33 (2H, q, J = 7.0 Hz, H-1""), 3.54 (2H, q, J = 7.0 Hz, CH_3–$\underline{CH_2}$–N), 3.90 (2H, q, J = 7.0 Hz, H-1""), respectively. A doublet of methyl appeared at δ 1.61 (3H, d, J = 7.0 Hz, H-3"') together with a quadrat at δ 4.62 (1H, q, J = 7.0 Hz, H-2"') was allotted to the sulfur-linked methine proton. The protons of azinane ring was resonated at δ 1.90–2.05 (4H, m, H-3',5'), 2.82 (1H, m, H-4'), 3.08 (2H, m, H-2',6') and 4.16 (2H, m, H-2',6'). Two triplets and a doublet displayed at δ 7.01 (1H, t, J = 8.0 Hz, H-4"), 7.26 (2H, t, J = 8.0 Hz, H-3",5") and 7.33 (2H, d, J = 8.0, H-2",6") assigned to the protons of monosubstituted phenyl group. The ^{13}C NMR spectra (BB and DEPT) showed a total of 21 carbon signals for 23 carbon nuclei, which endorsed the presence of four methyl, six methylene, four methine, and five quaternary carbon atoms. The upmost downfield peaks at δ 170.7, 157.4, 155.1, and 149.6 were consigned to two carbonyls of amide groups and two quaternary carbons of triazole, respectively. The resonances at δ 139.2, 129.0, 123.2, and 120.1 corroborated the presence of phenyl ring. The signals for three *N*-ethyl groups appeared at δ 43.8, 42.7, 41.0, 15.9, 14.9 and 12.9. Furthermore, the carbons of azinane ring reverberated at δ 44.0, 43.9, 32.8, 30.4 and 30.3. The molecular formula $C_{23}H_{33}N_6O_2S$ was figured through HR-EI-MS, which displayed the molecular ion $[M]^+$ peak at *m/z*

458.2483. The spectral data for the remaining compounds **7b-n** of the series is presented in the experimental section.

3.2. 15-LOX inhibitory activities and SAR studies

In our continual efforts in search for 15-LOX inhibitors as potential leads in the development of anti-inflammatory agents as reported in the preceding studies [53–56], the present work was designed to assess the inhibitory activities of newly synthesized 1,2,4-triazole derivatives (**7a-n**) towards soybean 15-LOX enzyme. The results displayed substantial inhibitory profiles as given in Table 2. Quercetin (IC_{50} 4.86 ± 0.14 μM) and baicalein (IC_{50} 2.24 ± 0.13 μM) were used as standards during these studies. These results demonstrate that the introduction of a methyl group to the carbon chain of the linker exaggerated the inhibitory potential of the synthesized compounds. All analogues except **7k** and **7m** (which were inactive) had enormous inhibitory potential (IC_{50} 0.36 ± 0.15 to 23.59 ± 0.24 μM) *en route* to 15-LOX (Table 2, Fig. 2).

Previous studies have revealed that molecules possessing the *m*-methyl substituent on the phenyl ring observed potent anti-LOX activity [56,63,64]. In the present studies, the analogues **7e, 7j, 7h, 7a, 7g, 7b, 7n** and **7c** showed the potent inhibitory activities with IC_{50} values 0.36 ± 0.15 μM, 0.48 ± 0.18 μM, 0.84 ± 0.15 μM, 2.65 ± 0.11 μM, 3.83 ± 0.13 μM, 4.93 ± 0.12 μM, 5.76 ± 0.14 μM and 6.75 ± 0.17 μM, respectively. The comparison of molecules **7a** and **7b** with analogues **7c-7n** possessing a non-aromatic substituent stipulates that the substituent on the phenyl ring has more influence on the inhibitory activity than the structural feature related to aromatized electrophilic substituent. As stated, the best inhibition potential was shown by compounds **7e, 7h** and **7j** possessing disubstituted and monosubstituted benzene ring demonstrating the electron donating effect of these groups to enhance the hydrophobic interactions established with the enzyme (Table 2, Fig. 2).

While comparing the inhibitory profiles of **7a** and **7b** (IC_{50} 2.65 ± 0.11 μM and IC_{50} 4.93 ± 0.12 μM, respectively) it is observed that the diethyl groups diffused greater electron donating effects that resulted in somewhat higher IC_{50} of **7b**. By evaluating the activity of **7f** (IC_{50} 15.54 ± 0.26 μM) and **7g** (IC_{50} 3.83 ± 0.13 μM), the same substituents (ethyl group) were attached at the *ortho* and *para* positions, respectively, which corroborated that the electron donating effect of ethyl group was more prominent at *para* position as compared to *ortho* position. The ethyl group enhanced the electron density on nitrogen atom to establish better π-π interaction for the active site of the enzyme. It is justified that the electron donating substituents augmented the prohibitory action of the drug candidate. However, the paradoxical values found in activity are due to the position of these groups, and the inhibitory action abates where their stearic obstruction is tyrannized as in **7i** (IC_{50} 21.56 ± 0.27 μM) and **7j** (IC_{50} 0.48 ± 0.18 μM) and **7l** (IC_{50} 12.15 ± 0.23 μM). The lower inhibitory potential of **7d** (IC_{50} 23.59 ± 0.24 μM) advocated that the electron releasing effect of methyl group at *meta* position was less as compared to *ortho* and *para* positions (Table 2, Fig. 2). Although, both analogues **7c** and **7n** displayed remarkable and comparable

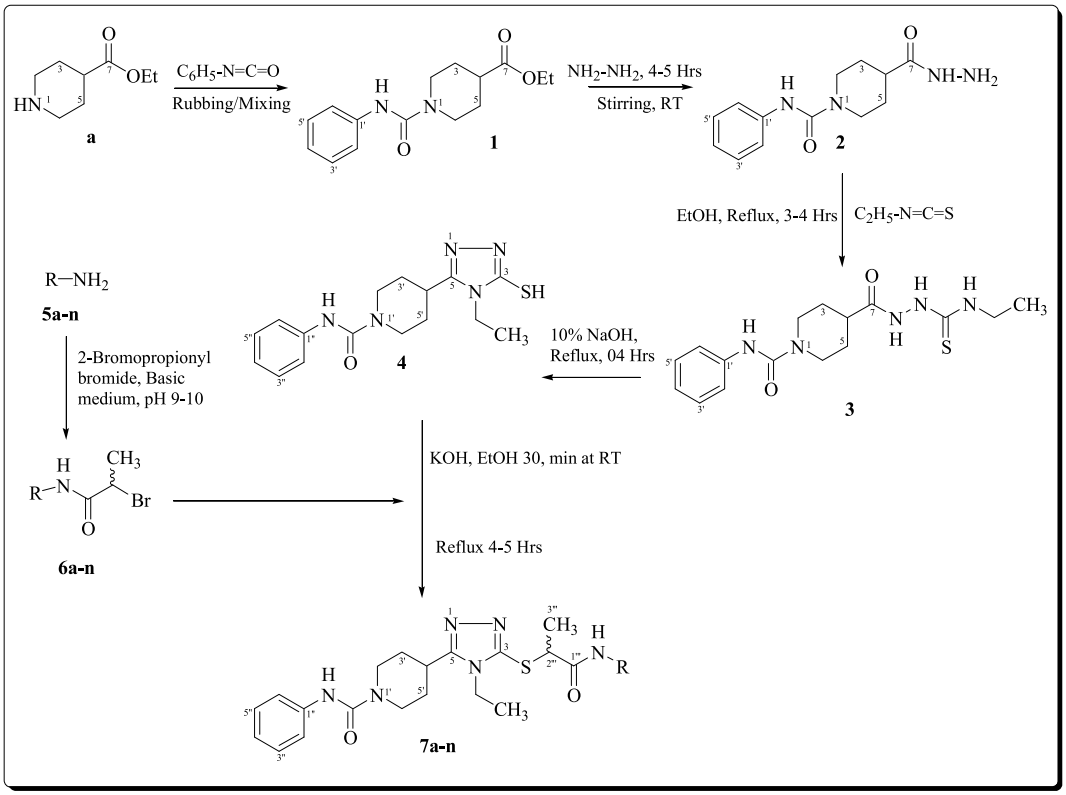

Scheme 1. Protocol for the synthesis of triazole amides (**7a-n**) from isonipecotate.

Table 1
Alkyl/aryl substituted amines.

Comp	R	Comp	R	Comp	R
a	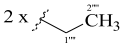	**f**	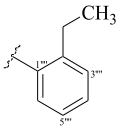	**k**	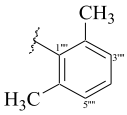
b	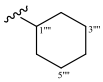	**g**	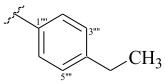	**l**	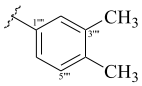
c	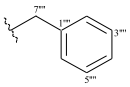	**h**	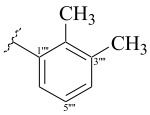	**m**	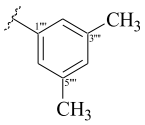
d	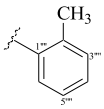	**i**	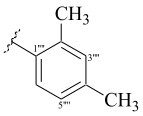	**n**	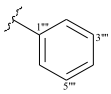
e	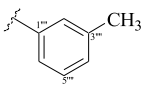	**j**	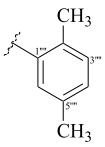		

inhibition properties (IC_{50} 6.75 ± 0.17 μM and 5.76 ± 0.14 μM), but the presence of methylene bridge between nitrogen and phenyl ring in former hampered the involvement of lone pair of nitrogen with phenyl ring by resonance that caused a trivial lack of inhibitory potential as reported earlier [53–56]. The results altogether infer that the nature along with the position of substituents attached to phenyl ring had great consequences on the enzyme inhibitory potential.

3.3. Cell viability studies

MTT assay was performed to determine the MNCs viability at 0.25 mM concentration. The results show that all the compounds maintained >75 % viability (Table 2). They observed less toxicity towards MNCs under the assay conditions as compared with the standard anticancer drugs at the same studied concentration.

Table 2
15-LOX inhibitory and cytotoxicity profiles of compounds **7a-n** (Mean ± SEM, n = 3).

Comp	15-LOX assay		MTT assay
	Inhibition (%) at 0.25 mM	IC_{50} (μM)	Cell viability (%) at 0.25 mM
7a	89.54 ± 1.24	2.65 ± 0.11	81.35 ± 2.8
7b	87.62 ± 1.27	4.93 ± 0.12	83.75 ± 2.9
7c	88.47 ± 1.23	6.75 ± 0.17	79.65 ± 2.8
7d	85.62 ± 1.47	23.59 ± 0.24	76.57 ± 2.7
7e	89.64 ± 1.23	0.36 ± 0.15	84.43 ± 2.9
7f	87.34 ± 1.34	15.54 ± 0.26	76.26 ± 2.8
7g	86.61 ± 1.23	3.83 ± 0.13	87.64 ± 2.6
7h	89.72 ± 1.35	0.84 ± 0.15	78.62 ± 2.8
7i	85.64 ± 1.46	21.56 ± 0.27	86.25 ± 2.7
7j	89.48 ± 1.28	0.48 ± 0.18	87.63 ± 2.9
7k	56.49 ± 1.59	>200	75.67 ± 2.8
7l	88.49 ± 1.25	12.15 ± 0.23	79.31 ± 2.9
7m	57.37 ± 1.46	>200	78.24 ± 2.7
7n	84.65 ± 1.29	5.76 ± 0.14	82.17 ± 2.9
Quercetin	96.63 ± 1.24	4.86 ± 0.14	–
Baicalein	93.79 ± 1.27	2.24 ± 0.13	–
Cyclophosphamide	–	–	58.45 ± 2.6
Cisplatin	–	–	57.34 ± 2.4
Curcumin	–	–	71.82 ± 2.8

3.4. ADME studies

The ADME (absorption, distribution, metabolism, elimination) properties of the analogues were determined by MedChem Designer 5.5. The results are mentioned in Table 3. For oral absorption of the drug, the drug solubility and absorption parameters are indicated in terms of their log values (MlogP, S + logP and S + logD). As per rule, the values of these parameters should be < 5.0 and all compounds exhibited good behavior towards these profiles.

As per Lipinski's/Veber rule, the M.W. should be ≤ 500 and eight compounds (**7f-m**) possessed M.W. slightly above 500 (MW 506.6) and is also acceptable under the rule. As per rule, the calculated number of rotatable bonds (M_NO) should be ≤ 10, and all analogues revealed the acceptable number of rotatable bonds. As per rule, the molecules should have polar surface area of (T_PSA) of ≤140 Å^2, and all compounds displayed these values in the limit. Lastly, the number of H-bond donors (HBDB) should be ≤ 5 and the sum of hydrogen bond donors and acceptors (M_NO + HBDH) should be ≤ 12 and both these parameters are within the drug-likeness properties of the compounds [63,64]. The data given in the Table overall reveals the good ADME properties without the violation of the Lipinski's/Veber rules.

3.5. Computational studies

Molecular docking of all the 1,2,4-triazole derivatives (**7a-n**) was performed using Autodock Vina [58]. The targeted protein crystal structure, 15-LOX from soybean (PDB ID: 1IK3, resolution: 2.0 Å), was downloaded from RCSB PDB [59]. Prior to docking procedures, the downloaded protein was prepared using Autodock Vina and visualized in Biovia Discovery studio [60]. All the hetero atoms including co-crystal ligand were removed. The protein crystal was protonated by adding polar hydrogen atoms and partial charges were added. After the preparation of both ligands and protein, all ligands were docked into the active pocket of 15-LOX protein using inbuilt united atom scoring function with 10 runs for each ligand. The protein active pocket is composed of amino acids residues which

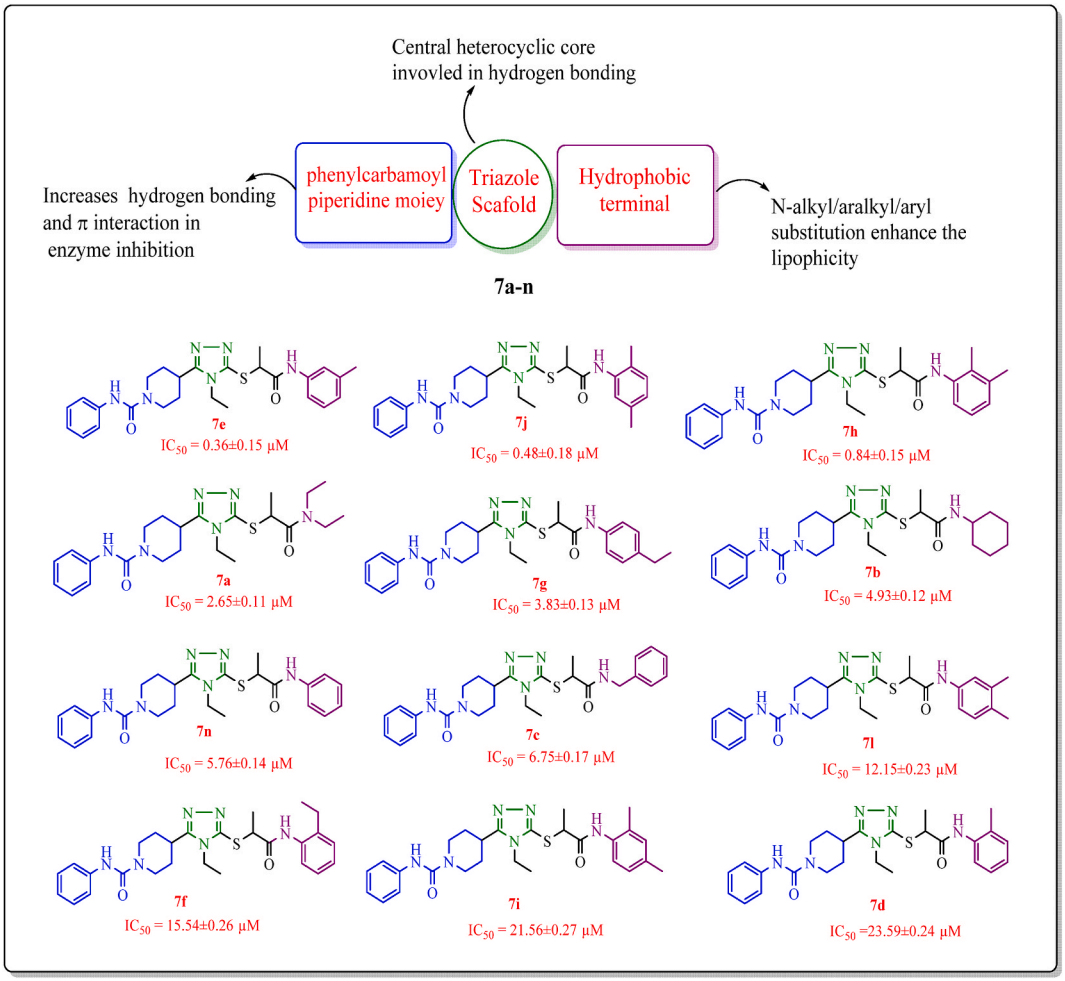

Fig. 2. SAR studies of 15-LOX inhibitors of the series **7a-n.**

included Glu197, Arg260, Val26, Asp25, Val256, Lys278, Leu560, Leu563, Ala263, Phe272, Gln598, Asp592, Lys388, Asp 603, Tyr512, Asp431, Leu729, Gln574, Pro759, Gln762, Phe761, Thr443, Gly579, Arg580, Ile440, Trp578. The active pocket was assumed to be static during rigid receptor docking, which allowed for extended contact time between specific amino acid residues and selected compounds [61]. Finally, 2D and 3D poses were generated and further analyzed.

3.5.1. Molecular docking studies

The soybean 15-LOX is a large protein with an oblong shape and several domains that wrap around single-nuclear heme iron active sites (Fig. 3). The beta barrel domain and primary catalytic site make up active 15-LOX. The hydrophobic residues that make up its C-terminal domain constitute the substrate binding site. When the substrate binds to hydrophobic residues, inflammatory processes may be triggered and the potential targets for docking at the binding site include these hydrophobic amino acid residues (Fig. 3).

The results of docking studies are highly consistent with the *in vitro* activities. The most active analogues **7e**, **7h** and **7j** exhibited the most potent and stable interactions with the highest docking scores compared to the other compounds against 15-LOX protein. The docking results augmented the anti-LOX potential of **7e**, **7h** and **7j** analogues (Table 4).

3.5.2. Binding interactions of potent derivatives

The docking results of all the derivatives (**7a-n**) including their binding interactions and binding free energies were determined and the 2D, 3D poses of the most potent compounds are shown below (Figs. 4–6). The compound **7e** displayed various stable bonding and non-bonding interactions with the amino acid residues of the active pocket, i.e., Gln598, Asp592, Lys388, Asp 603, Tyr512, Asp431 and observed binding free energy of −9.20 kcal/mol. Among all the bonding interactions, one conventional hydrogen bond and one carbon hydrogen bond is formed by Gln598 and Asp 592 with the carbonyl oxygen atom and tolylamino ring. Three π-anion bonds are formed with the amino acids Asp431, Asp592 and Asp603. The first two π-anion bonds are formed with the tolylamino ring and 3rd bond is formed with the piperidine ring. Nevertheless, other alkyl and π-alkyl bonds are also formed by the amino acids Lys388 and Tyr512 (Table 4, Fig. 4).

Likewise, the docking interaction of compound **7h** are comparatively more stable and extended which included Arg260, Val26, Glu197, Asp25, Val256, Lys278, Leu560, Leu563, Ala263, Phe272, Lys591, Arg386 (Fig. 5). The higher binding free energy of −9.70 kcal/mol of **7h** may be attributed to the substitution of additional methyl group at tolylamino ring forming dimethylphenyl amino ring which enhanced the resulted stability of the compound. The bonding interactions of **7h** also include two conventional hydrogen bonds, one carbon hydrogen bond, two π-anion bonds, one π-π stacked bond and five weak alkyl interactions. The two hydrogen bonds are formed by the amino acid Arg260 and Val26 with the nitrogen atom of triazole ring and carbonyl oxygen atom attached to dimethylphenyl amino ring which also forms the conventional hydrogen bond with amino acid Asp25. The π-anionic bonds are formed by Glu197 and Lys278 with the 2nd nitrogen of triazole ring and piperidine ring. All other amino acids are involved in forming weak alkyl and π-alkyl associations (Fig. 5).

The binding free energy of **7j** was found the highest among the series, i.e., −9.8 kcal/mol which is almost equal to the compound **7h** and may be attributed to the striking structural similarity. The position of 2nd methyl group on the same ring is slightly changed in **7j** which lead to most potent bonding interactions. The bonding and non-bonding interactions include two conventional hydrogen bonds, two carbon hydrogen bonds, one π-donor hydrogen bond, one π-δ bond, two π-stacked bond and various alkyl and π-alkyl interactions. The amino acids involved in bonding interactions are Leu729, Pro759, Phe761, Gly579, Ile440, Trp578, Gln762, Gln574, Thr443, Arg580 (Fig. 6). The amino acid Gln762 forms two conventional hydrogen bonds with the nitrogen atom of triazole ring and carbonyl oxygen attached to diphenyl amino ring. The other three hydrogen bonds are formed by the amino acids Arg580, Thr443 and Gln574, i.e., two with the piperidine ring and one with the ring adjacent to the piperidine ring. The only π-δ bond is formed by Gly579 with

Table 3
Calculated ADME properties of the analogues (**7a-n**)[a].

Comp	MlogP	S + logP	S + logD	M. W.	M_NO	T_PSA	HBDH	nVs
Lipinski/Veber	**≤ 5**	**≤ 5**	**≤ 5**	**≤ 500**	**≤ 10**	**≤ 140 Å^2**	**≤ 5**	**≤ 1**
7a	2.950	2.593	2.593	458.629	8	83.360	1	0
7b	3.369	3.216	3.216	484.667	8	92.150	2	0
7c	3.346	2.765	2.765	492.647	8	92.150	2	0
7d	3.614	3.315	3.315	492.647	8	92.150	2	0
7e	3.614	3.384	3.384	492.647	8	92.150	2	0
7f	3.815	3.696	3.696	506.674	8	92.150	2	1
7g	3.815	3.803	3.803	506.674	8	92.150	2	1
7h	3.815	3.633	3.633	506.674	8	92.150	2	1
7i	3.815	3.690	3.690	506.674	8	92.150	2	1
7j	3.815	3.687	3.686	506.674	8	92.150	2	1
7k	3.815	3.596	3.596	506.674	8	92.150	2	1
7l	3.815	3.719	3.719	506.674	8	92.150	2	1
7m	3.815	3.739	3.739	506.674	8	92.150	2	1
7n	3.410	3.045	3.045	478.620	8	92.150	2	0
Quercetin	−0.235	1.958	1.529	302.242	7	131.36	5	0
Baicalein	1.296	3.019	2.823	270.243	5	90.900	3	0

[a] **Footnote:** MlogP: Lipophilicity, M_NO: No. of rotatable bonds, T_PSA: Molecular polar surface area, HBDH: No. of H-bond donors, nV: No. of rule violations.

piperidine ring suggesting the role in the stabilization of this ring. The π-stacked bonds are formed by Phe761 and Trp578 with both terminal rings, that is, diphenylamine ring and piperidine ring. The alkyl and π-alkyl bonds are formed by amino acids Leu729, Pro759 and Ile440. The docking results of all the derivatives suggest that substitution of methyl group at the diphenylamino ring enhances the stability and anti-LOX properties of the compounds.

3.6. Density functional theory calculations

DFT calculations play pivotal role in drug discovery because of the lower computational cost and reliable predictions. The present investigations projected the electrophilic and nucleophilic features, hardness and softness properties and reactivity potential in intra- and intermolecular interactions (Supplementary file). The descriptors related with the DFT calculations are described below.

3.6.1. Frontier molecular orbitals

The energy of frontier molecular orbitals, i.e., highest occupied molecular orbital (HOMO) and lowest unoccupied molecular orbital (LUMO) of any compound are used to estimate various chemical properties associated with the electronic distribution. Any compound with high value of HOMO appears to be good electron donor and in the same way higher LUMO value are shown by electron acceptors. The overall calculation of these orbitals helps in the determination of local reactivity at different sites in a compound. The difference between HOMO and LUMO energy of a compound is an important reflection of its reactivity profile. Any compound with higher energy gap tends to be the least reactive which is represented by its high hardness value. According to these results, the compound **7m** appears to be highly reactive which is evident from its lowest energy gap, i.e., $\Delta Egap = -0.157$ eV. The energy gap for all the other compound is positive and is given along with other parameters (Table 5).

The dipole moment of any compound is associated with the charge segregation in a molecule and represents the behavior of reactive sites. The highest value of dipole moment for **7f,** i.e., 9.05 D and the lowest for **7d** represents its relative charge separation in the molecule. Polarizability, dipole moment, energy of HOMO and LUMO orbitals along with their relative energy gap and structures of HOMO and LUMO orbitals for the most potent compounds are described and are given in Figs. 7–8.

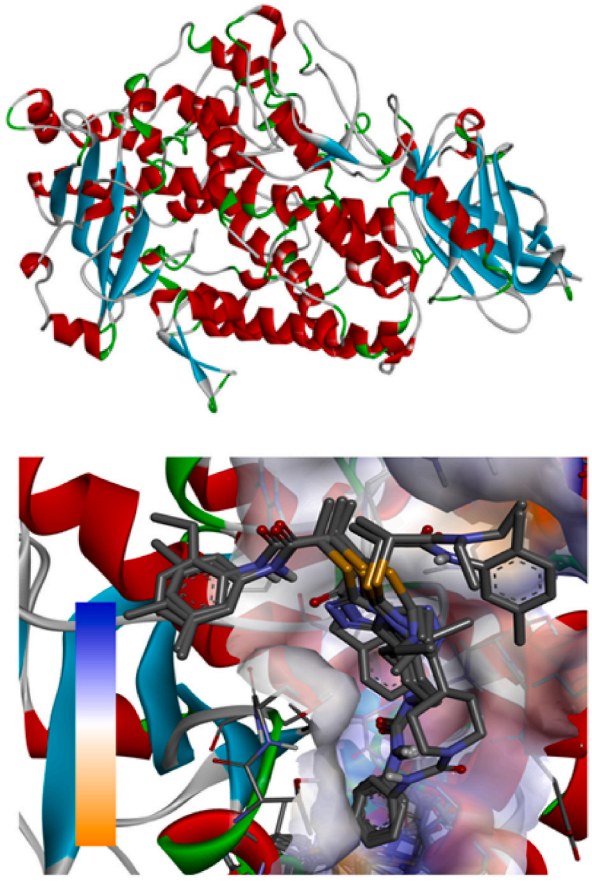

Fig. 3. Crystal structure of protein 15-LOX (PDB ID: 1IK3) (above) and the docked conformations of active ligand-protein complexes (below).

Table 4
Binding free energies and molecular binding interactions observed by potent ligand-protein complexes.

Comp	Binding free energy (kcal/mol)	Interaction type	Amino acid residues	RMSD (Å)
7a	−7.72	Hydrogen Bonding Hydrophobic interactions	Gln762, Gln5574, Thr443 Phe761, Pro759, Ile440, Gly579, Tpr578	1.24
7b	−8.12	Hydrogen bonding Hydrophobic interactions	No hydrogen Bond Leu426, Leu376, Tyr512, Arg378	0.73
7c	−7.80	Hydrogen Bonding Hydrophobic interactions	Gln762, Ser444, Thr443, Arg580 Leu729, Gly579, Ile440, Trp578	1.54
7d	−8.42	Hydrogen Bonding Hydrophobic interactions	No hydrogen Bond Leu376, Tyr512, Leu426	1.90
7e	−9.20	Hydrogen Bonding Hydrophobic interactions	Gln598 Asp592, Lys388, Asp 603, Tyr512, Asp431	1.47
7f	−8.22	Hydrogen Bonding Hydrophobic interactions	Arg731, Gln574, Arg580, Thr443 Lys755, Arg732, Leu729, Gly579, Trp578, Ile440	1.52
7g	−8.24	Hydrogen Bonding Hydrophobic interactions	Arg260, Val26 Glu197, Lys278, Val256, Leu563, Phe272	1.71
7h	−9.70	Hydrogen bonding Hydrophobic interactions	Arg260, Val26 Glu197, Asp25, Val256, Lys278, Leu560, Leu563, Ala263, Phe272, Lys591, Arg386	1.98
7i	−8.52	Hydrogen Bonding Hydrophobic interactions	Arg378, Asp428 Leu380, Pro385, Lys388, Asp603	0.94
7j	−9.8	Hydrogen Bonding Hydrophobic interactions	Gln762, Gln574, Thr443, Arg580 Leu729, Pro759, Phe761, Gly579, Ile440, Trp578	0.81
7k	−8.52	Hydrogen Bonding Hydrophobic interactions	Asp428 Leu426, Tyr512, Leu376, Tyr512	1.51
7l	−8.42	Hydrogen Bonding Hydrophobic interactions	Gln574, Thr443, Arg580 Ile440, Trp578, Gly579, Leu729, Arg731, Pro759	1.68
7m	−8.72	Hydrogen Bonding Hydrophobic interactions	Arg731, Gln574, Thr443, Arg580 Leu729, Pro759, Arg732, Gly579, Trp578	1.96
7n	−8.22	Hydrogen Bonding Hydrophobic interactions	Asp428 Leu426, Val589, Tyr512, Leu376	1.36
Quercetin	−8.47	Hydrogen bonding Hydrophobic interactions	Arg389, Asp608, Lys388, Asn375 Val589, Asp592, Asp390, Asp428, Leu380	1.13
Baicalein	−8.98	Hydrogen bonding Hydrophobic interactions	Asp431, Arg378, Leu376 Val594, Trp593, Leu520, Tyr512, Val589, Gln598, Cys379	1.53

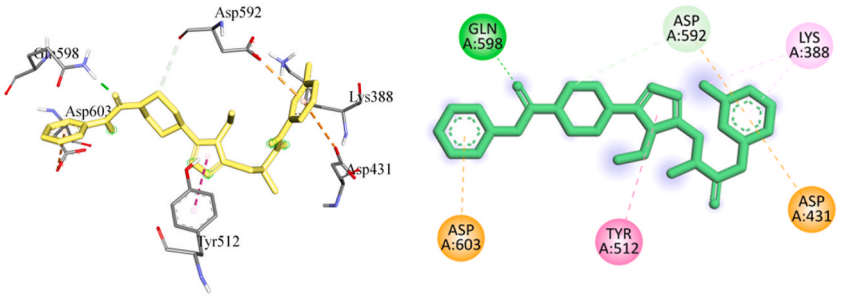

Fig. 4. 2D and 3D binding interactions of **7e** with in the active pocket of 15-LOX.

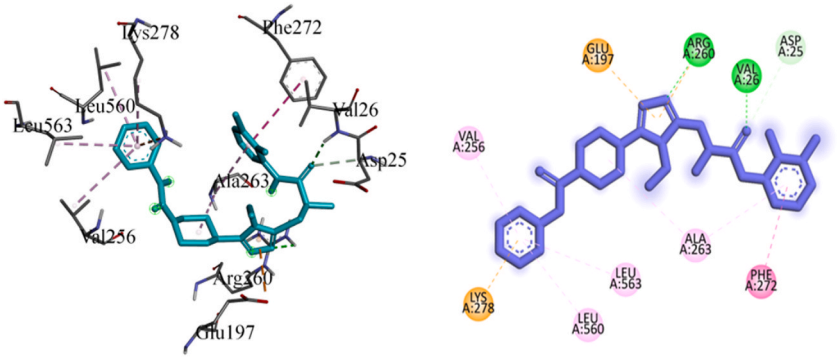

Fig. 5. 2D and 3D binding interactions of **7h** with in the active pocket of 15-LOX.

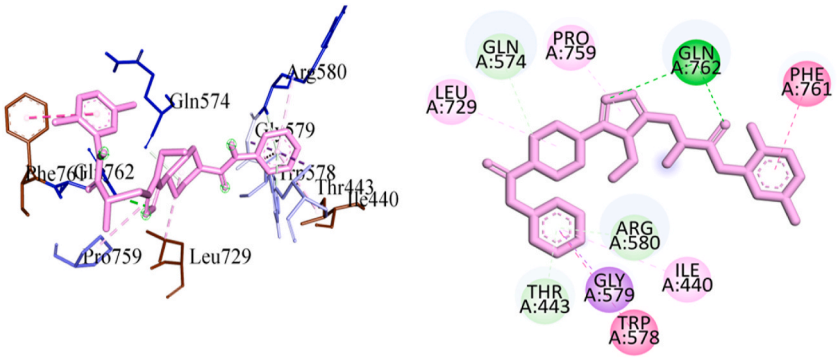

Fig. 6. 2D and 3D binding interactions of **7j** with in the active pocket of 15-LOX.

3.6.2. Chemical descriptors

Chemical hardness, chemical softness, electronegativity, electrophilicity index, and electronic chemical potential are various parameters used to determine the reactivity of a compound. The reactivity and stability of a chemical system serves as indicators of its chemical hardness which is calculated by chemical formula (ELUMO-EHOMO)/2). The ability of an atom to attract electrons is measured by its electronegativity, which is the ability of an atom in a molecule to draw electrons towards itself, i.e., X = - (EHOMO + ELUMO)/2). The ability of a molecule to receive electrons utilizing its chemical hardness and electronic chemical potential is known as its electrophilicity index. The values of various chemical descriptors for all the compounds were found comparable and are given in the Table 6 below.

Table 5
Optimization energies, HOMO and LUMO energies and energy gap values of compounds (**7a-n**).

Comp	Optimization Energy	Dipole Moment	Polarizability (α)	EHOMO (eV)	ELUMO (eV)	EHOMO-LUMO (Δ eV)
7a	−1773.66	5.81	312.34	−0.209	−0.019	0.190
7b	−1851.08	4.99	331.40	−0.210	−0.022	0.188
7c	−1886.76	4.84	336.25	−0.216	−0.210	0.006
7d	−1886.76	3.47	341.64	−0.216	−0.211	0.005
7e	−1886.77	3.95	346.37	−0.211	−0.038	0.173
7f	−1925.90	9.05	358.45	−0.210	−0.021	0.189
7g	−1926.07	4.33	360.46	−0.218	−0.037	0.181
7h	−1926.07	7.54	352.51	−0.216	−0.028	0.188
7i	−1926.07	3.91	355.87	−0.219	−0.036	0.183
7j	−1926.07	3.76	354.84	−0.211	−0.037	0.174
7k	−1926.07	4.02	352.46	−0.210	−0.033	0.177
7l	−1926.07	4.39	360.80	−0.217	−0.036	0.181
7m	−1926.07	4.23	359.41	−0.212	−0.369	−0.157
7n	−1847.46	3.80	333.57	−0.217	−0.039	0.178

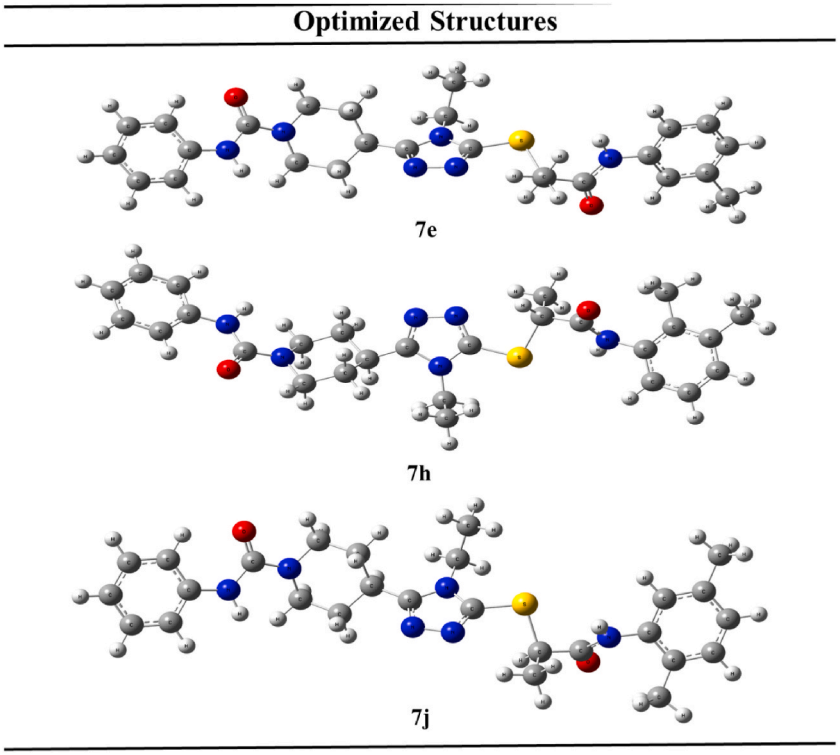

Fig. 7. The optimized structures of three active compounds **7e, 7h** and **7j**.

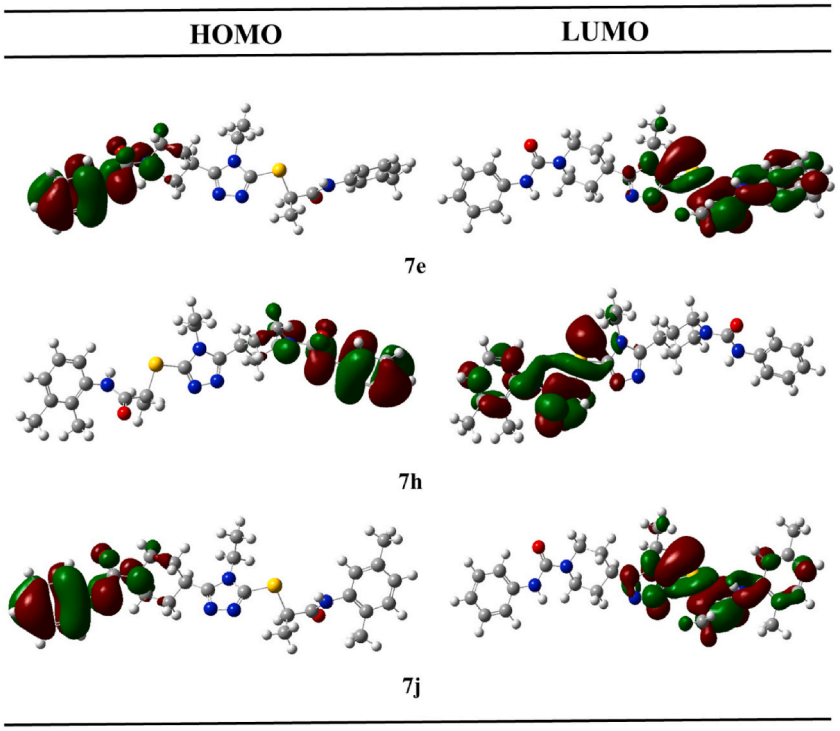

Fig. 8. The HOMO and LUMO illustrations of three active compounds **7e, 7h** and **7j**.

Table 6
Various chemical descriptors the compounds **7a-n**.

Comp	Chemical Potential (μ, eV)	Electronegativity (X, eV)	Hardness (η, eV)	Softness (S, eV^{-1})	Electrophilicity Index (ω, eV)
7a	−0.114	0.114	0.095	5.260	0.068
7b	−0.116	0.116	0.094	5.320	0.072
7c	−0.213	0.213	0.003	166.67	7.561
7d	−0.214	0.214	0.003	200.00	9.116
7e	−0.125	0.125	0.087	5.780	0.090
7f	−0.116	0.116	0.095	5.290	0.071
7g	−0.128	0.128	0.091	5.520	0.090
7h	−0.122	0.122	0.094	5.320	0.079
7i	−0.128	0.128	0.092	5.460	0.089
7j	−0.124	0.124	0.087	5.750	0.088
7k	−0.122	0.122	0.089	5.650	0.083
7l	−0.127	0.127	0.091	5.520	0.088
7m	−0.291	0.291	−0.079	−6.370	−0.538
7n	−0.128	0.128	0.089	5.620	0.092

4. Conclusions

In conclusion, a series of *N*-alkyl/aralkyl/aryl derivatives (**7a-n**) of 4-(5-mercapto-4-phenyl-4H-1,2,4-triazol-3-yl)-*N*-phenyl-piperdine-1-carboxamide was designed, synthesized, characterized and screened against 15-LOX. Eight compounds disclosed potent inhibitory profiles with IC_{50} values < 7 μM (**7e, 7j, 7h, 7a, 7g, 7b, 7n, 7c**), two compounds (**7l, 7f**) displayed IC_{50} values < 16 μM, two compounds (**7i, 7d**) observed IC_{50} values (21.56 ± 0.27 μM, 23.59 ± 0.24 μM) and 2 compounds (**7k, 7m**) were found inactive against the 15-LOX enzyme. SAR studies revealed that the nature and the position of substituents bonded to phenyl ring greatly [65] affected the inhibitory potential of the enzyme. These compounds demonstrated least toxicity towards MNCs as determined by MTT assay. ADME properties predicted good lipophilicity, bioavailability, drug-likeness properties and other physicochemical properties of the analogues. These *in vitro* studies were supported by molecular docking studies. Molecular docking studies revealed binding free energy values lower than the standard quercetin and baicalein with RMSD <2.0 (Å). The amino acids Gln598 (**7e**, RMSD 1.47), Arg260, Val 126 (**7h**, RMSD 1.98) and Gln762, Gln574, Thr443, Arg580 (**7j,** RMSD 0.81) established hydrogen bonding with the ligands and hydrophobic interactions stabilized the protein ligand interactions. DFT calculations established that species with more stabilized LUMO had higher enzyme inhibitory potential. Further investigations are warranted in search for leads as 15-LOX inhibitors.

CRediT authorship contribution statement

Zahid Nawaz: Writing – original draft, Data curation. **Naheed Riaz:** Writing – review & editing, Investigation, Conceptualization. **Muhammad Saleem:** Writing – review & editing, Formal analysis. **Ambar Iqbal:** Methodology, Formal analysis. **Syeda Abida Ejaz:** Validation, Methodology. **Saima Muzaffar:** Methodology, Data curation. **Bushra Bashir:** Investigation, Formal analysis, Data curation. **Muhammad Ashraf:** Writing – review & editing, Supervision, Investigation. **Aziz-ur Rehman:** Project administration, Methodology, Conceptualization. **Muhammad Sajjad Bilal:** Investigation, Formal analysis, Data curation. **Bala Krishna Prabhala:** Software, Data curation. **Salvia Sajid:** Resources, Formal analysis.

Declaration of competing interest

We are submitting a manuscript entitled "**Probing *N*-Substituted 4-(5-mercapto-4-ethyl-4H-1,2,4-triazol-3-yl)-*N*-phenyl-piperdine-1-carboxamides as potent 15-LOX inhibitors** supported **with ADME, DFT calculations and molecular docking studies**", for publication in Heliyon. We are not or will not submit the same results to any other journal for publication till the final decision from the subject journal. None of the authors have any conflict of interest.

Appendix A. Supplementary data

Supplementary data to this article can be found online at https://doi.org/10.1016/j.heliyon.2024.e35278.

References

[1] H. Kuhn, S. Banthiya, K.V. Leyen, Mammalian lipoxygenases and their biological relevance, BBA 1851 (2015) 308–330, https://doi.org/10.1016/j.bbalip.2014.10.002.
[2] T. Wang, X. Fu, Q. Chen, J.K. Patra, D. Wang, Z. Wang, Z. Gai, Arachidonic acid metabolism and kidney inflammation, Int. J. Mol. 20 (2019) 3683, https://doi.org/10.3390/ijms.20153683.
[3] A. Orafaie, M.M. Matin, H. Sadeghian, The importance of 15-lipoxygenase inhibitors in cancer treatment, Cancer Metastasis 37 (2–3) (2018) 397–408, https://doi.org/10.1007/s10555-018-9738-9.

[4] A.D. Dobrian, M.A. Morris, D.A. Taylor-Fishwick, T.R. Holman, Y. Imai, R.G. Mirmira, J.L. Nadler, Role of the 12-lipoxygenase pathway in diabetes pathogenesis and complications, Pharmacol. Ther. 195 (2019) 100–110, https://doi.org/10.1016/j.pharmthera.2018.10.010.

[5] H.W. Gardner, Recent investigations into the lipoxygenase pathway in plants, BBA 1084 (1991) 221–239, https://doi.org/10.1016/0005-2760(91)90063-N.

[6] A. Liavonchanka, I. Feussner, Lipoxygenases: occurrence, functions and catalysis, J. Plant Physiol. 163 (2006) 348–357, https://doi.org/10.1016/j.jplph.2005.11.006.

[7] H. Sadeghian, A. Jabbari, 15-Lipoxygenase inhibitors: a patent review, Expert Opin. Ther. Pat. 26 (2016) 65–88, https://doi.org/10.1517/13543776.2016.1113259.

[8] A.D. Dobrian, D.C. Lieb, B.K. Cole, D.A. Taylor-Fishwick, S.K. Chakrabarti, L. Nadler, Functional and pathological roles of the 12-and 15-lipoxygenases, Prog. Lipid Res. 50 (2011) 115–131, https://doi.org/10.1016/j.plipres.2010.10.005.

[9] P. Lu, M.L. Schraq, D.E. Slaughter, C.E. Raab, Mechanism based inhibition of human liver microsomal cytochrome P450 1A2 by Zileuton, a 5-lipoxygenase inhibitor, Drug Metab. Dispos. 31 (2003) 1352–1360, https://doi.org/10.1124/dmd.31.11.1352.

[10] C. Hu, S. Ma, Recent development of lipoxygenase inhibitors as anti-inflammatory agents, Med. Chem. Comm. 9 (2018) 212–225, https://doi.org/10.1039/C7MD00390K.

[11] S. Sinha, M. Doble, S.L. Manju, 5-Lipoxygenase as a drug target: a review on trends in inhibitors structural design, SAR and mechanism-based approach, Bioorg. Med.Chem. 27 (2019) 3745–3759, https://doi.org/10.1016/j.bmc.2019.06.040.

[12] E. Skrzypczak-Jankun, J. Chorostowska-Wynimko, S.H. Selman, J. Jankun, Lipoxygenases – a challenging problem in enzyme inhibition and drug development, Curr. Enzyme. Inhib. 3 (2007) 119–132, https://doi.org/10.2174/157340807780598350.

[13] M.M. Heravi, V. Zadsirjan, Prescribed drugs containing nitrogen heterocycles: an overview, RSC Adv. 10 (2020) 44247–44311, https://doi.org/10.1039/D0RA09198G.

[14] B.F. Abdel-Wahab, S. Shaaban, G.A. El-Hiti, Synthesis of sulfur-containing heterocycles via ring enlargement, Mol. Divers. 22 (2018) 517–542, https://doi.org/10.1007/s11030-017-9810-3.

[15] N.K. Verma, D. Mondal, S. Bera, Pharmacological and cellular significance of triazole-surrogated compounds, Curr. Org. Chem. 23 (2019) 2505–2572, https://doi.org/10.2174/1385272823666191021114906.

[16] R. Aggarwal, G. Sumran, An insight on medicinal attributes of 1,2,4-triazoles, Eur. J. Med. Chem. 205 (2020) 1–46, https://doi.org/10.1016/j.ejmech.2020.112652.

[17] V. Mikhailo, S. Natalia, I. Korol, M. Maksym, Fused bicyclic 1,2,4-triazoles with one extra sulfur atom: synthesis, properties, and biological activity, J. Heterocyclic Chem. (2020) 1–9, https://doi.org/10.1002/jhet.4044.

[18] D. Kumudha, R.R. Reddy, T. Kalavathi, 1,2,4-Triazoles: as biological important agents, Int. J. Pharm. Sci. Res. 3 (2012) 4562–4572, https://doi.org/10.13040/IJPSR.0975.

[19] R. Kharb, P.C. Sharma, M.S. Yar, Pharmacological significance of triazole scaffold, J. Enzyme. Inhib. Med. Chem. 26 (2011) 1–21, https://doi.org/10.3109/14756360903524304.

[20] P. Kaur, A. Chawla, 1,2,4-Triazole: a review of pharmacological activities, Int. Res. J. Pharm. 8 (2017) 10–29, https://doi.org/10.7897/2230-8407.087112.

[21] S. Maddila, R. Pagadala, S.B. Jonnalagadda, 1,2,4-Triazoles: a review of synthetic approaches and the biological activity, Lett. Org. Chem. 10 (2013) 693–714, https://doi.org/10.2174/15701786101013126115448.

[22] C.H. Zhou, Y. Wang, Recent researches in triazole compounds as medicinal drugs, Curr. Med. Chem. 19 (2012) 239–280, https://doi.org/10.2174/092986712803414213.

[23] A. Abdelli, S. Azzouni, R. Plais, A. Gaucher, M. Efrit, D. Prim, Recent advances in the chemistry of 1,2,4-triazoles: synthesis, reactivity and biological activities, Tetrahedron Lett. 86 (2021) 153518, https://doi.org/10.1016/j.tetlet.2021.153518.

[24] G. Nistor, M. Mioc, A. Mioc, M. Balan-Porcarasu, R. Racoviceanu, A. Prodea, A. Milan, R. Ghiulai, A. Semenescu, C. Dehelean, C. Soica, The C30-modulation of betulinic acid using 1,2,4-triazole: a promising strategy for increasing its antimelanoma cytotoxic potential, Molecules 27 (2022) 7807, https://doi.org/10.3390/molecules27227807.

[25] J. Zhang, S. Wang, Y. Ba, Z. Xu, 1,2,4-Triazole-quinoline/quinolone hybrids as potential anti-bacterial agents, Eur. J. Med. Chem. 174 (2019) 1–8, https://doi.org/10.1016/j.ejmech.2019.04.033.

[26] J. Xu, Y. Cao, J. Zhang, S. Yu, Y. Zou, X. Chai, Q. Sun, Design, synthesis and antifungal activities of novel 12,4-triazole derivatives, Eur. J. Med. Chem. 46 (2011) 3142–3148, https://doi.org/10.1016/j.ejmech.2011.02.042.

[27] G.S. Kumar, Y. Rajendraprasad, B.P. Mallikarjuna, S.M. Chandrashekar, C. Kistayya, Synthesis of some novel 2-substituted-5-[isopropylthiazole] clubbed 1,2,4-triazole and 1,3,4-oxadiazoles as potential antimicrobial and antitubercular agents, Eur. J. Med. Chem. 45 (2010) 2063–2074, https://doi.org/10.1016/j.ejmech.2010.01.045.

[28] Z. Peng, G. Wang, Q.H. Zeng, Y. Li, Y. Wu, H. Liu, Y. Zhao, Synthesis, antioxidant and anti-tyrosinase activity of 1,2,4-triazole hydrazones as antibrowning agents, Food Chem. 341 (2021) 128265, https://doi.org/10.1016/j.foodchem.2020.128265.

[29] R.R. Radwan, N.H. Zaher, M.G. El-Gazzar, Novel 1,2,4-triazole derivatives as antitumor agents against hepatocellular carcinoma, Chem. Biol. Interact. 274 (2017) 68–79, https://doi.org/10.1016/j.cbi.2017.07.008.

[30] F. Ahmadi, M.R. Ghayahbashi, M. Sharifzadeh, E. Alipoiur, S.N. Ostad, M. Vosooghi, M. Amini, Synthesis and evaluation of anti-inflammatory and analgesic activities of new 1,2,4-triazole derivatives, Med. Chem. 11 (2015) 69–76, https://doi.org/10.2174/1573406410666140613154507.

[31] R. Paprocka, M. Wiese, A. Eljaszewicz, A. Helmin-Basa, A. Gzella, B. Modzelewska-Banachiewicz, J. Michalkiewicz, Synthesis and anti-inflammatory activity of new 1,2,4-triazole derivatives, Bioorg. Med. Chem. 25 (2015) 2664–2667, https://doi.org/10.1016/j.bmcl.2015.04.079.

[32] F. Zhao, Y. Liu, Z. Qin, Y. Wu, Y. Xiao, J.Q. Li, Synthesis and insecticidal activity of novel 1,2,4-triazole containing amidine moiety, J. Heter. Chem. 59 (2022) 1723–1735, https://doi.org/10.1002/jhet.4500.

[33] S. Rani, K. Raheja, V. Luxami, K. Paul, A review on diverse heterocyclic compounds as the privileged scaffolds in non-steroidal aromatase inhibitors, Bioorg. Chem. 113 (2021) 105017, https://doi.org/10.1016/j.bioorg.2021.105017.

[34] L. Gavara, F. Verdirosa, L. Sevaille, A. Legru, G. Corsica, L. Nauton, P. Mercuri, F. Sannio, F. De Luca M. Hadjadj, G. Cerboni, Y. Hoang, P. Licznar-Fajardo, M. Galleni, J. Docquier, J. Hernandez, 1,2,4-Triazole-3-thione analogues with an arylakyl group at position 4 as metallo-β-lactamase inhibitors, Bioorg. Med. Chem. 72 (2022) 116964, https://doi.org/10.1016/j.bmc.2022.116964.

[35] K. Abdellatif, E. Abdelall, H. Elshemy, J. Philoppes, E. Hassanein, N. Kahk, Optimization of pyrazole-based compounds with 1,2,4-triazole-3-thiol moiety as selective COX-2 inhibitors cardioprotective drug candidates: design, synthesis, cyclooxygenase inhibition, anti-inflammatory, ulcerogenicity, cardiovascular evaluation, and molecular modeling studies, Bioorg. Chem. 114 (2021) 105122, https://doi.org/10.1016/j.bioorg.2021.105122.

[36] R. Adiguzel, F. Turkan, U. Yildiko, A. Aras, E. Evren, T. Onkol, Synthesis and in silico studies of novel Ru(II) complexes of Schiff base derivatives of 3-[(4-amino-5-thioxo-1,2,4-triazole-3-yl)methyl]-2(3H)-benzoxazolone compounds as potent glutathione S-transferase and cholinesterases inhibitor, J. Mol. Struct. 1231 (2021) 129943, https://doi.org/10.1016/j.molstruc.2021.129943.

[37] H. Uslu, D. Osmaniye, B. Saglik, S. Levent, Y. Ozkay, K. Benkli, Z. Kaplancikli, Design, synthesis, in vitro, and in silico studies of 1,2,4-triazole-piperazine hybrid derivatives as potential MAO inhibitors, Bioorg. Chem. 117 (2021) 105430, https://doi.org/10.1016/j.bioorg.2021.105430.

[38] I. Khan, M. Hanif, M. Hussain, A. Khan, M. Aslam, N. Rama, J. Iqbal, Synthesis, acetylcholinesterase and alkaline phosphatase inhibition of some new 1,2,4-triazole and 1,3,4-thiadiazole derivatives, Aust. J. Chem. 65 (2012) 1413–1419, https://doi.org/10.1071/CH12134.

[39] P. Channar, A. Saeed, A. Larik, S. Rashid, Q. Iqbal, M. Rozi, J. Mahar, Design and synthesis of 2,6-di(substituted phenyl)thiazolo[3,2-b]-1,2,4-triazoles as α-glucosidase and α-amylase inhibitors, co-relative pharmacokinetics and 3D QSAR and risk analysis, Biomed. Pharmacother. 94 (2017) 499–513, https://doi.org/10.1016/j.biopha.2017.07.139.

[40] E. Yeye, K. Khan, S. Chigurupati, A. Wadood, A. Rehman, S. Perveen, M. Taha, Synthesis, in vitro α-amylase and α-glucosidase dual inhibitory activities of 4-amino-1,2,4-triazole derivatives their molecular docking and kinetic studies, Bioorg. Med. Chem. 28 (2020) 115467, https://doi.org/10.1016/j.bmc.2020.115467.

[41] F. Hichri, A. Omri, A. Hossan, H.B. Jannet, Alpha-glucosidase and amylase inhibitory effects of Eruca vesicaria subsp. longirostris essential oils: synthesis of new 1,2,4-triazole-thiol derivatives and 1,3,4-thiadiazole with potential inhibitory activity, Pharm. Biol. 57 (2019) 564–570, https://doi.org/10.1080/13880209.2019.1642363.

[42] E. Mentese, S. Ulker, B. Kahveci, Synthesis and study of α-glucosidase inhibitory, antimicrobial and antioxidant activities of some benzimidazole derivatives containing triazole, thiadiazole, oxadiazole, and morpholine rings, Chem. Heter. Comp. 50 (2015) 1671–1682, https://doi.org/10.1007/s10593-015-1637-1.

[43] P. Goel, O. Alam, M.J. Naim, F. Nawaz, M. Iqbal, M.I. Alam, Recent advancement of piperidine moiety in treatment of cancer-A review, Eur. J. Med. Chem. 157 (2018) 480–502, https://doi.org/10.1016/j.ejmech.2018.08.017.

[44] A. Ashraf, A. Hassan, M.M. Makhlouf, S. Brase, Chemistry and biological activities of 1,2,4-triazolethiones-antiviral and anti-infective drugs, Molecules 25 (2020) 1–54, https://doi.org/10.3390/molecules25133036.

[45] S.T. Harini, H.V. Kumar, J. Rangaswamy, N. Naik, Synthesis, antioxidant and antimicrobial activity of novel vanillin derived piperidin-4-one oxime esters: preponderant role of the phenyl ester substituents on the piperidin-4-one oxime core, Bioorg. Med. Chem. Let. 22 (24) (2012) 7588–7592, https://doi.org/10.1016/j.bmcl.2012.10.019.

[46] M.B. Tehrani, S. Emami, M. Asadi, M. Saeedi, M. Mirzahekmati, S.M. Ebrahimi, A. Shafiee, Imidazo[2,1-b]thiazole derivatives as new inhibitors of 15-lipoxygenase, Eur. J. Med. Chem. 87 (2014) 759–764, https://doi.org/10.1016/j.ejmech.2014.10.011.

[47] M.A. Abdelgawad, M.B. Labib, M. Abdel-Latif, Pyrazole-hydrazone derivatives as anti-inflammatory agents: design, synthesis, biological evaluation, COX-1, 2/5-LOX inhibition and docking study, Bioorg. Chem. 74 (2017) 212–220, https://doi.org/10.1016/j.bioorg.2017.08.014.

[48] P. Srivastava, V.K. Vyas, B. Variya, P. Patel, G. Qureshi, M. Ghate, Synthesis, anti-inflammatory, analgesic, 5-lipoxygenase (5-LOX) inhibition activities, and molecular docking study of 7-substituted coumarin derivatives, Bioorg. Chem. 67 (2016) 130–138, https://doi.org/10.1016/j.bioorg.2016.06.004.

[49] H.S. El-Bordiny, M.M. El-Miligy, S.E. Kassab, H. Daabees, W.A.M. Ali, S.A.M. El-Hawash, Design, synthesis, biological evaluation and docking studies of new 3-(4,5-dihydro-1H-pyrazol/isoxazol-5-yl)-2-phenyl-1H-indole derivatives as potent antioxidants and 15-lipoxygenase inhibitors, Eur. J. Med. Chem. 145 (2018) 594–605, https://doi.org/10.1016/j.ejmech.2018.01.026.

[50] H.S. Lee, A. Abdildinova, Y.S. Cho, H.G. Cheon, Y.D. Gong, A novel core skeleton design and synthesis of N-alkyl-1′-(substitutedsulfonyl)spiro[chromene-2,4′-piperidin]-6-amine derivatives as 5-lipoxygenase inhibitors, BKCS 43 (2022) 801–813, https://doi.org/10.1002/bkcs.12520.

[51] B. Jiang, X. Huang, H. Yao, J. Jiang, X. Wu, S. Jiang, J. Xu, Discovery of potential anti-inflammatory drugs: diaryl-1,2,4-triazoles bearing N-hydroxyurea moiety as dual inhibitors of cyclooxygenase-2 and 5-lipoxygenase, Org. Biomol. Chem. 12 (2014) 2114–2127, https://doi.org/10.1039/C3OB41936C.

[52] T. Asghari, M. Bakavoli, H. Eshghi, S. Saberi, Z. Ebrahimpour, Synthesis of 5,5′-(ethane-1,2-diyl)bis(3-((5-bromo-6-methyl-2-tertiaryaminopyrimidin-4-yl)thio)-4H-1,2,4-triazol-4-amines) and their novel bis-cyclized products, 1,2-bis(pyrimido[5,4e][1,2,4]triazolo[3,4-b][1,3,4]thiadiazin-3-yl)ethane, as potential inhibitors of 15-lipoxygenase, J. Heter. Chem. 53 (2016) 403–407, https://doi.org/10.1002/jhet.2421.

[53] B. Bashir, W. Shahid, M. Ashraf, M. Saleem, Aziz-ur Rehman, S. Muzaffar, M. Imran, H. Amjad, K. Bhattarai, N. Riaz, Identification of phenylcarbamoylazinane-1,3,4-oxadiazole amides as lipoxygenase inhibitors with expression analysis and computational studies, Bioorg. Chem. 115 (2021) 105243, https://doi.org/10.1016/j.bioorg.2021.105243.

[54] N. Riaz, M. Yasin, M. Ashraf, M. Saleem, B. Bashir, A. Iqbal, Aziz-ur Rehman, S.A. Ejaz, H.M.K. Mahmood, K. Bhattarai, Vetting of new N-furfurylated p-chlorophenyl-1,2,4-triazole acetamides as lipoxygenase inhibitors assisted with in vitro and in silico studies, J. Iran. Chem. Soc. 20 (2023) 977–994, https://doi.org/10.1007/s13738-022-02733-2.

[55] B. Bashir, N. Riaz, S.A. Ejaz, M. Saleem, A. Iqbal, M. Ashraf, Aziz-ur Rehman, M. Aziz, K. Bhattarai, Contemplation of p-tolyloxy-1,3,4-oxadiazole propionamides as 15-lipoxygenase inhibitors in succoring with in vitro and in silico studies, J. Biomol. Struct. Dyn. 41 (2023) 1–20, https://doi.org/10.1080/07391102.2023.2190807.

[56] S. Muzaffar, W. Shahid, N. Riaz, M. Saleem, M. Ashraf, Aziz-ur Rehman, B. Bashir, A. Kaleem, M. al-Rashida, B. Baral, K. Bhattarai, H. Gross, Probing phenylcarbamoylazinane-1,2,4-triazole amides derivatives as lipoxygenase inhibitors along with cytotoxic, ADME and molecular docking studies, Bioorg. Chem. 108 (2021) 104525, https://doi.org/10.1016/j.bioorg.2020.104525.

[57] W. Shahid, M. Ashraf, M. Saleem, B. Bashir, S. Muzaffar, M. Ali, A. Kaleem, Aziz-ur Rehman, H. Amjad, K. Bhattarai, N. Riaz, Exploring phenylcarbamoylazinane-1,2,4-triazole thioethers as lipoxygenase inhibitors supported with expression analysis, cellular viability and in silico studies, Bioorg. Chem. 115 (2021) 105261, https://doi.org/10.1016/j.bioorg.2021.105261.

[58] O. Trott, A.J. Olson, AutoDock Vina, Improving the speed and accuracy of docking with a new scoring function, efficient optimization, and multithreading, J. Comput. Chem. 31 (2010) 455–461, https://doi.org/10.1002/jcc.21334.

[59] L.I. Design, Pharmacophore and Ligand-Based Design with Biovia Discovery Studio®, Biovia, California, 2014.

[60] M.O. Taha, M. Habash, Z. Al-Hadidi, A. Al-Bakri, K. Younis, S. Sisan, Docking-based comparative intermolecular contacts analysis as new 3-D QSAR concept for validating docking studies and in silico screening: NMT and GP inhibitors as case studies, J. Chem. Inf. Model. 51 (2011) 647–669, https://doi.org/10.1021/ci100368t.

[61] M.J. Frisch, G.W. Trucks, H.B. Schlegel, G.E. Scuseria, M.A. Robb, J.R. Cheeseman, G. Scalmani, V. Barone, B. Mennucci, G.A. Petersson, H. Nakatsuji, M. Caricato, X. Li, H.P. Hratchian, A.F. Izmaylov, J. Bloino, G. Zheng, J.L. Sonnenberg, M. Hada, M. Ehara, K. Toyota, R. Fukuda, J. Hasegawa, M. Ishida, T. Nakajima, Y. Honda, O. Kitao, H. Nakai, T. Vreven, J.A. Montgomery, J.E. Peralta, M.J. Ogliaro, J. Bearpark, E.N. Heyd, K.N. Brothers, V.N. Kudin, R. Staroverov, F. Kobayashi, J. Normand, K. Raghavachari, A.P. Rendell, J.C. Burant, S.S. Iyengar, J. Tomasi, M. Cossi, N. Rega, N.J. Millam, M. Klene, J.E. Knox, J.B. Cross, V. Bakken, C. Adamo, J. Jaramillo, R. Gomperts, R.E. Stratmann, O. Yazyev, A.J. Austin, R. Cammi, C. Pomelli, J.W. Ochterski, R.L. Martin, K. Morokuma, V.G. Zakrzewski, G.A. Voth, P. Salvador, J.J. Dannenberg, S. Dapprich, A.D. Daniels, O. Farkas, J.B. Foresman, J.V. Ortiz, J. Cioslowski, D.J. Fox, Gaussian 09 (D01), Inc., Wallingford, CT, USA, 2010.

[62] K. Bhavani, S. Renuga, S. Muthu, Quantum mechanical study and spectroscopic (FT-IR, FT-Raman, ^{13}C, ^{1}H) study, first order hyperpolarizability, NBO analysis, HOMO and LUMO analysis of 2-acetoxybenzoic acid by density functional methods, Spectrochimica Acta Part A, Mol. Biomol. Spectrosc. 136 (2015) 1260–1268, https://doi.org/10.1016/j.saa.2014.10.012.

[63] C.A. Lipinski, F. Lombardo, B.W. Dominy, P.J. Feeney, Experimental and computational approaches to estimate solubility and permeability in drug discovery and development settings, Adv. Drug Deliv. Rev. 23 (1–3) (1997) 3–25, https://doi.org/10.1016/j.addr.2012.09.019.

[64] D.F. Veber, S.R. Johnson, H.Y. Cheng, B.R. Smith, K.W. War, K.D. Kopple, Molecular properties that influence the oral bioavailability of drug candidates, J. Med. Chem. 45 (12) (2002) 2615–2623, https://doi.org/10.1021/jm020017n.

[65] Y.M. Omar, S.G. Abdel-Moty, H.H.M. Abdu-Allah, Further insight into the dual COX-2 and 15-LOX anti-inflammatory activity of 1,3,4-thiadiazole-thiazolidinone hybrids: the contribution of the substituents at 5th positions is size dependent, Bioorg. Chem. 97 (2020) 103657, https://doi.org/10.1016/j.bioorg.2020.103657.